Electronic Supplementary Material (ESI) for Catalysis Science & Technology.

Supporting Information

Mononuclear Fe in N-doped carbon: computational elucidation of active sites for electrochemical oxygen reduction and oxygen evolution reactions

Rui Shang[1,2,3], Stephan N. Steinmann[4], Bo-Qing Xu[1*], Philippe Sautet[2,3*]

[1]Innovative Catalysis Program, Key Lab of Organic Optoelectronics & Molecular Engineering,
Department of Chemistry, Tsinghua University, Beijing 100084, China
[2]Department of Chemical and Biomolecular Engineering, University of California Los Angeles,
Los Angeles, CA 90095, United States
[3]Department of Chemistry and Biochemistry, University of California Los Angeles,
Los Angeles, CA 90095, United States
[4]Univ Lyon, Ecole Normale Supérieure de Lyon, CNRS Université Lyon 1, Laboratoire de Chimie
UMR 5182, 46 allée d'Italie, F-69364, Lyon, France

Figures

Fig. S1 The geometry of different cluster models (L-FeN_x, x = 2 or 4, L = nothing, O or OH). Grey, blue, orange, red and white spheres represent C, N, Fe, O and H atoms, respectively.

Fig. S2 Free energy diagrams of FeN_4 periodic model for ORR with different methods. Three multiplicities (singlet, triplet and quintet) have been considered for intermediate *O and two multiplicities (doublet and quartet) have been considered for intermediate *OH and *OOH. (a) PBE, (b) PBE with Van der Waals interaction, (c) PBE in implicit solvent and (d) PBE with Van der Waals interaction in implicit solvent.

Fig. S3 Free energy diagrams of FeN_4 periodic model on ORR with different methods. The energy diagrams are based on the most stable spin state for each intermediate. (a) PBE, (b) PBE with Van der Waals interaction, (c) PBE in implicit solvent and (d) PBE with Van der Waals interaction in implicit solvent.

Fig. S4 Free energy diagrams for ORR assuming (a) FeN_4, (b) FeN_2-trans and (c) FeN_2-cis as active sites in PBE (left), with Van der Waals interaction included (middle) and in implicit solvent (right) in periodic models with CHE approach at equilibrium potential (1.23 V). Intermediate structures of O=FeN_x or HO-FeN_x (x=2 or 4) are also considered as active sites to start a second ORR cycle as shown with the red and blue lines and labels, respectively.

Fig. S5 The geometry of (a) O=FeN_2-cis-O and (b) O=FeN_2-trans-O from top view and side view. Grey, blue, orange, red and white spheres represent C, N, Fe, O and H atoms, respectively.

Fig. S6 Free energy diagrams for ORR assuming (a) FeN_4, (b) FeN_2-trans and (c) FeN_2-cis as active sites in PBE (left), in PBE, PBE with Van der Waals interaction, PBE in implicit solvent and PBE with Van der Waals interaction in implicit solvent (from left to right) in cluster models with CHE approach at equilibrium potential (1.23 V). Intermediate structures of O=FeN_x or HO-FeN_x (x=2 or 4) are also considered as active sites to start a second ORR cycle as shown with the red and blue lines and labels, respectively.

Fig. S7 The adsorption free energy difference of (a) OOH, (b) O and (c) OH on both periodic and cluster models with PBE results as the reference. The column bar in light red, orange and blue stands for results with Van der Waals interaction, implicit solvent and both effects included, respectively. The column bar in shadow and blank stands for the periodic and cluster models, respectively.

Fig. S8 Free energy diagrams for OER assuming (a) FeN_4, (b) FeN_2-trans and (c) FeN_2-cis as active sites in PBE, PBE with Van der Waals interaction, PBE in implicit solvent and PBE with Van der Waals interaction in implicit solvent (from left to right) with CHE approach at equilibrium potential (1.23 V). Intermediate structures of HO-FeN_x or O=FeN_x (x=2 or 4) are also considered as active sites to start a second OER cycle as shown with the blue and red lines and labels, respectively.

Fig. S9 The geometry for FeN_4, HO-FeN_4 and HO-FeN_2-cis. Grey, blue, orange, red and white spheres represent C, N, Fe, O and H atoms, respectively

Fig. S10 The fitted G(V) parabola as a function of potential. (a) bare surface, (b) *OOH, (c) *O and (d) *OH on FeN_4.

Fig. S11 The electronic charges as a function of potential. (a) bare surface, (b) *OOH, (c) *O and (d) *OH on FeN_4.

Fig. S12 The fitted G(V) parabola as a function of potential. (a) bare surface, (b) *OOH, (c) *O and (d) *OH on HO-FeN_4.

Fig. S13 The electronic charges as a function of potential. (a) bare surface, (b) *OOH, (c) *O and (d) *OH on HO-FeN_4.

Fig. S14 The fitted G(V) parabola as a function of potential. (a) bare surface, (b) *OOH, (c) *O and (d) *OH on HO-FeN_2-cis.

Fig. S15 The electronic charges as a function of potential. (a) bare surface, (b) *OOH, (c) *O and (d) *OH on HO-FeN_2-cis.

Fig. S16 The difference in free energy of elementary steps between SC and CHE approaches on FeN_4 (black), HO-FeN_4 (red) and HO-FeN_2-cis (blue) as a function of difference in workfunction at 0.0 charge. Four elementary steps in ORR are shown by square, circle, triangle and inverted triangle in sequence. The energy for SC is chosen at the 0.0 V and which is chosen at 0.0 charge for CHE.

Fig. S17 Top view and side view of spin density on (a) bare FeN_4 active site (b) *OOH (c) *O and (d) *OH in periodic models at isosurface level 0.005, where light blue represents negative and yellow represents positive spin density. Different spin states were considered for the bare site and intermediates. Grey, blue, orange, red and white spheres represent C, N, Fe, O and H atoms, respectively.

Fig. S18 Top view and side view of spin density on (a) bare FeN_2–trans active site (b) *OOH (c) *O and (d) *OH in periodic models at isosurface level 0.005, where light blue represents negative and yellow represents positive spin density. Different spin states were considered for the bare site and intermediates. Grey, blue, orange, red and white spheres represent C, N, Fe, O and H atoms, respectively.

Fig. S19 Top view and side view of spin density on (a) bare FeN_2-cis active site (b) *OOH (c) *O and (d) *OH in periodic models at isosurface level 0.005, where light blue represents negative and yellow represents positive spin density. Different spin states were considered for the bare site and intermediates. Grey, blue, orange, red and white spheres represent C, N, Fe, O and H atoms, respectively.

Fig. S20 Top view and side view of spin density on (a) *OOH (b) *O (c) *OH of O=FeN_4 active sites, (d) *OOH (e) *O (f) *OH of O=FeN_2-trans active sites and (g) *OOH (h) *O (i) *OH of O=FeN_2-cis active sites in periodic models at isosurface level 0.005, where light blue represents negative and yellow represents positive spin density. Different spin states were considered for the bare site and intermediates. Grey, blue, orange, red and white spheres represent C, N, Fe, O and H atoms, respectively.

Fig. S21 Top view and side view of spin density on (a) *OOH (b) *OH of HO-FeN_4 active sites, (c) *OOH (d) *OH of HO-FeN_2-trans active sites and (e) *OOH (f) *OH of HO-FeN_2-cis active site in periodic models at isosurface level 0.005, where light blue represents negative and yellow represents positive spin density. Different spin states were considered for the bare sites and intermediates. Grey, blue, orange, red and white spheres represent C, N, Fe, O and H atoms, respectively.

Fig. S22 Top view and side view of spin density on (a) bare FeN_4 active site (b) *OOH (c) *O and (d) *OH in cluster models at isosurface level 0.005, where light blue represents negative and yellow represents positive spin density. Different spin states were considered for the bare site and intermediates. Grey, blue, orange, red and white spheres represent C, N, Fe, O and H atoms, respectively.

Fig. S23 Top view and side view of spin density on (a) bare FeN_2–trans active site (b) *OOH (c) *O and (d) *OH in cluster models at isosurface level 0.005, where light blue represents negative and yellow represents positive spin density. Different spin states were considered for the bare site and intermediates. Grey, blue, orange, red and white spheres represent C, N, Fe, O and H atoms, respectively.

Fig. S24 Top view and side view of spin density on (a) bare FeN_2-cis active site (b) *OOH (c) *O and (d) *OH in cluster models at isosurface level 0.005, where light blue represents negative and yellow represents positive spin density. Different spin states were considered for the bare site and intermediates. Grey, blue, orange, red and white spheres represent C, N, Fe, O and H atoms, respectively.

Fig. S25 Top view and side view of spin density on (a) *OOH (b) *O (c) *OH of O=FeN_4 active sites, (d) *OOH (e) *O (f) *OH of O=FeN_2-trans active sites and (g) *OOH (h) *O (i) *OH of O=FeN_2-cis active sites in cluster models at isosurface level 0.005, where light blue represents negative and yellow represents positive spin density. Different spin states were considered for the bare site and intermediates. Grey, blue, orange, red and white spheres represent C, N, Fe, O and H atoms, respectively.

Fig. S26 Top view and side view of spin density on (a) *OOH (b) *OH of HO-FeN_4 active sites, (c) *OOH (d) *OH of HO-FeN_2-trans active sites and (e) *OOH (f) *OH of HO-FeN_2-cis active site in cluster models at isosurface level 0.005, where light blue represents negative and yellow represents positive spin density. Different spin states were considered for the bare sites and intermediates. Grey, blue, orange, red and white spheres represent C, N, Fe, O and H atoms, respectively.

Fig. S27 Potential scaling relations as a function of OH adsorption free energy for ORR (left) and potential scaling relations as a function of the difference between O and OH adsorption free energy for OER (right) with different methods applied. The energies are based on the most stable spin state of each intermediate for periodic (empty symbols) and cluster (solid symbols) models. The square, the circle and the triangle symbols stand for the FeN_x, HO-FeN_x (x=2 or 4) and O=FeN_4, respectively. (a) PBE, (b) PBE with Van der Waals interaction and (c) PBE in implicit solvent.

Tables

Computational Details

Methods

The elementary steps of oxygen reduction reaction (ORR) and oxygen evolution reaction (OER) are shown separately in equations 1-4 and equations 5-8 in acidic condition (* represents the “bare” catalytic active site and *OOH, *OH and *O indicate the site with a chemisorbed OOH, OH or O fragment, respectively):

1) $* + O_2 + H^+ + e^- \rightarrow *OOH$
2) $*OOH + H^+ + e^- \rightarrow *O + H_2O$
3) $*O + H^+ + e^- \rightarrow *OH$
4) $*OH + H^+ + e^- \rightarrow H_2O + *$
5) $H_2O + * \rightarrow *OH + H^+ + e^-$
6) $*OH \rightarrow *O + H^+ + e^-$
7) $*O + H_2O \rightarrow *OOH + H^+ + e^-$
8) $*OOH \rightarrow * + O_2 + H^+ + e^-$

The adsorption free energies of the intermediates were calculated according to the following equations 9-11 using H_2 and H_2O as energy references. The smaller the value of the adsorption free energies are, the stronger the adsorption is.

9) $\Delta G_{*OOH} = G_{*OOH} + 3/2G_{H2} - G_{*} - 2G_{H2O}$
10) $\Delta G_{*O} = G_{*O} + G_{H2} - G_{*} - G_{H2O}$
11) $\Delta G_{*OH} = G_{*OH} + 1/2G_{H2} - G_{*} - G_{H2O}$

In the framework of CHE approach, the energy of H^+ and e^- pairs were considered as the energy of 1/2 H_2. While in the framework of SC approach, the energies of each intermediate was selected at a specific potential. The free energies of elementary steps were calculated as equations 12-15 for ORR and equations 16-19 for OER.

12) $\Delta G_1 = \Delta G_{*OOH} - 4.92$ (ORR)
13) $\Delta G_2 = \Delta G_{*O} - \Delta G_{*OOH}$
14) $\Delta G_3 = \Delta G_{*OH} - \Delta G_{*O}$
15) $\Delta G_4 = -\Delta G_{*OH}$
16) $\Delta G_1 = \Delta G_{*OH}$ (OER)
17) $\Delta G_2 =\Delta G_{*O} - \Delta G_{*OH}$
18) $\Delta G_3 = \Delta G_{*OOH} - \Delta G_{*O}$
19) $\Delta G_4 = 4.92 -\Delta G_{*OOH}$

ΔU_1 to ΔU_4 were used to represent the potential can be generated from each step of ORR when $\Delta G_i = 0$, which was calculated as equations 20-23. The least generated potential will be the limiting potential for the reaction.

20) $\Delta U_1 = -(\Delta G_{*OOH} - 4.92) / e$

21) $\Delta U_2 = -(\Delta G_{*O} - \Delta G_{*OOH}) / e$

22) $\Delta U_3 = -(\Delta G_{*OH} - \Delta G_{*O}) / e$

23) $\Delta U_4 = (\Delta G_{*OH}) / e$

For the free energy calculation, the zero-point energies were included in all intermediates and molecules. The entropy contribution was dominated by the translational and rotational terms for gas phase and liquid phase molecules, and only entropic contributions from these molecules were included. The entropy data for gas-phase molecules were obtained from NIST database. The calculation for liquid phase water entropy was based on consideration of the equilibrium with a vapor pressure at 298K. The equations for calculating free energies of elementary steps are the same in acidic or basic condition.

The least exothermic step is the potential-determining step in ORR, while the largest endothermic step is the potential-determining step in OER. The overpotential could be obtained by accounting the deviation between the limiting potential and the equilibrium potential (1.23 V), which was defined as $\eta = E^o - (-\max(\Delta G_n)) / e$ in ORR and $\eta = (\max(\Delta G_n)) / e - E^o$ in OER[1]. The experimental equilibrium potential was used to evaluate the overpotential. If the DFT calculated value with PBE was used instead (1.14 V), then all ORR overpotentials were decreased by 0.10 V and all OER overpotentials were increased by the same value.

Supplementary Discussion

Intermediates in different spin states

Take the FeN_4 as an example, both of the bare active site and the intermediate *O can adopt a singlet, triplet or quintet spin state, while the intermediates *OH and *OOH are either in the doublet or quartet state. With the OOH or OH adsorbate on Fe, the doublet is more stable than quartet. The energy differences between doublet and quartet are 0.39 eV and less than 0.1 eV for OOH and OH, respectively. With O adsorbed, the triplet is the most stable spin state, then follows the singlet and quartet, having the same sequence as the bare active site.

For a dedicate understanding of the location of unpaired electrons, the spin density of bare active sites and intermediates in different spin states are shown in Fig. S17 – S26 and their magnetic moment of Fe and O are listed in Table S6-S11 for both periodic and cluster models. The intermediates prefer to stay in the low spin states. The unpaired electrons are located around Fe with the absence of adsorbate or ligand, and are located around Fe and O for intermediates or with an oxyl ligand. When the intermediates are in high spin states, the unpaired electrons will be delocalized on carbon.

Scaling relations on ORR and OER

The obtained volcano plot is very similar when performing a plain PBE computation, neglecting Van der Waals interaction and solvation effect (Fig. S27 and Table S15), with almost the same minimal overpotential in ORR. Even though OH adsorption is strengthened by 0.15 to 0.20 eV from Van der Waals interaction and solvation effect, the obtained scaling relations of the first step remain almost unchanged, but computed points move along these lines. The linear relation has, therefore, a universal character, but the position of the various actives sites on the volcano and the sites that optimize the limiting potential depend on the method. A similar small variation of the scaling relations[2] was observed earlier in the case of the energy difference between OOH and OH adsorption energies on precious metal surface when changing the exchange correlation functional.

The universal character was also observed in OER, if Van der Waals interaction and solvation effect are not considered, again the lines barely change, but in contrast to ORR, the point positions remain almost unchanged since the energy descriptor is a difference. Hence the inclusion or exclusion of Van der Waals interaction and solvation effect gives very similar results for OER.

Comparison between CHE and SC approaches

The disagreement between CHE and SC can be predicted from the analysis that the influence of the potential can be connected with the changes in the workfunction. Under the CHE approach, the electrochemical potential is assumed to affect only the chemical potential of the exchanged electrons. Thus, the electronic energy is independent with respect to the potential and taken from the neutral systems. However, the free energy for the sites and the intermediates in the "neutral" situation is not exactly the same as the U = 0.0 V situation. The change in workfunction between the system at 0.0 charge and at 0.0 V vs SHE reflects how much the SC approach will influence the system's energy (Fig. S16). The larger the variation in work function between steps, the larger the difference between the two approaches. The slope is similar for the -OH ligand containing sites (around 0.37), but is smaller for the FeN_4 site (around 0.17).

Both of ΔG_2 (circle symbols) and ΔG_3 (triangle symbols) points are clustered at the lower left and upper right zones where larger workfunction differences are observed. However, ΔG_1 (square symbols) and ΔG_4 (inverse triangle symbols) are gathered around in relative focused zone with smaller workfunction differences observed, indicating minor changes within the involved intermediates.

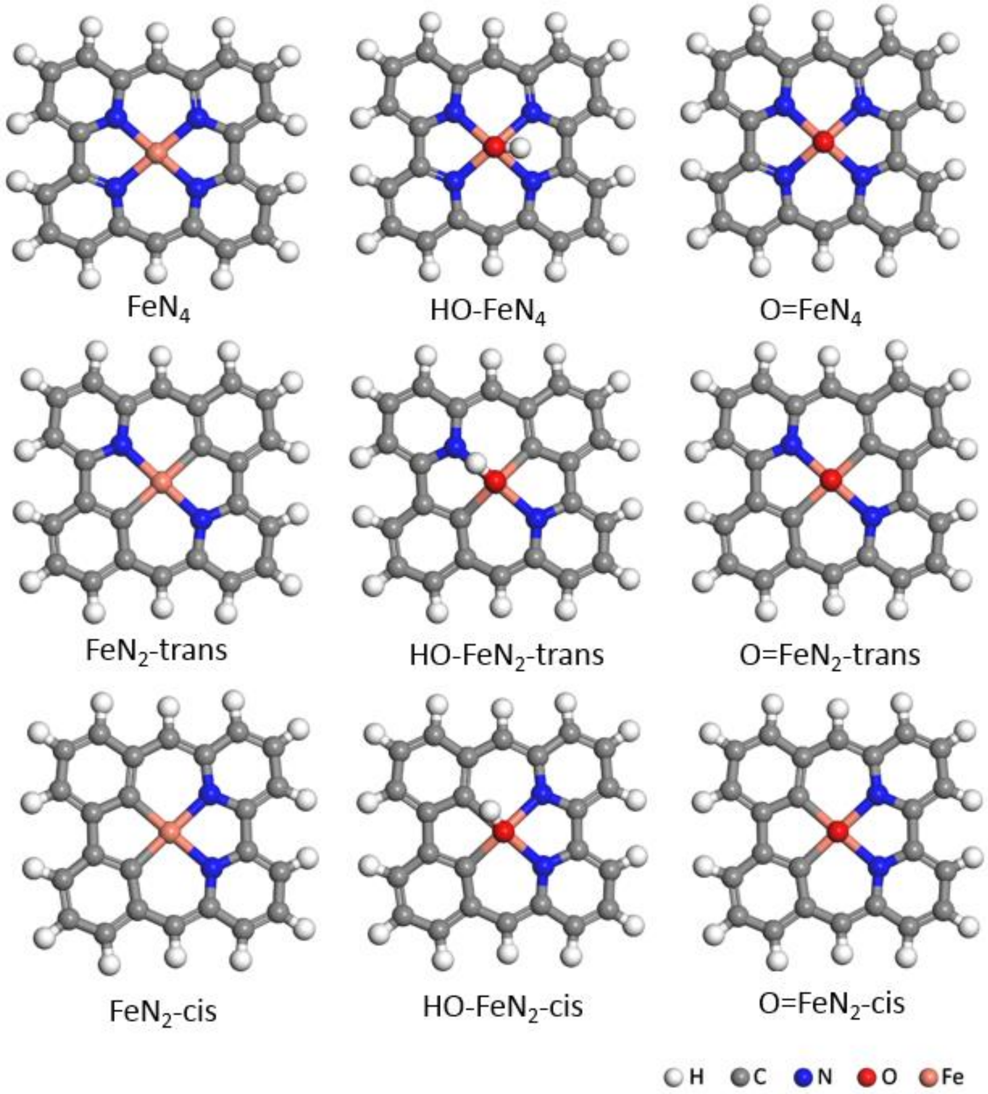

Fig. S1 The geometry of different cluster models (L-FeN$_x$, x = 2 or 4, L = nothing, O or OH). Grey, blue, orange, red and white spheres represent C, N, Fe, O and H atoms, respectively.

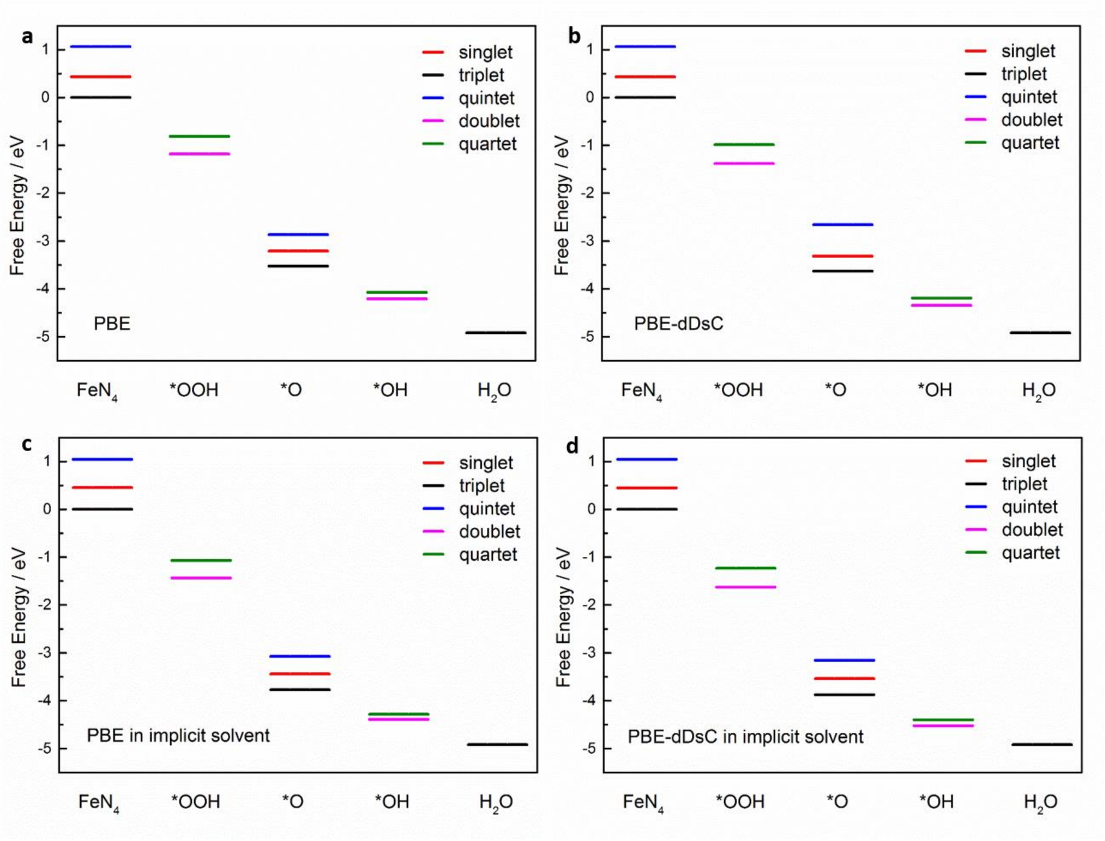

Fig. S2 Free energy diagrams of FeN_4 periodic model for ORR with different methods. Three multiplicities (singlet, triplet and quintet) have been considered for intermediate *O and two multiplicities (doublet and quartet) have been considered for intermediate *OH and *OOH. (a) PBE, (b) PBE with Van der Waals interaction, (c) PBE in implicit solvent and (d) PBE with Van der Waals interaction in implicit solvent.

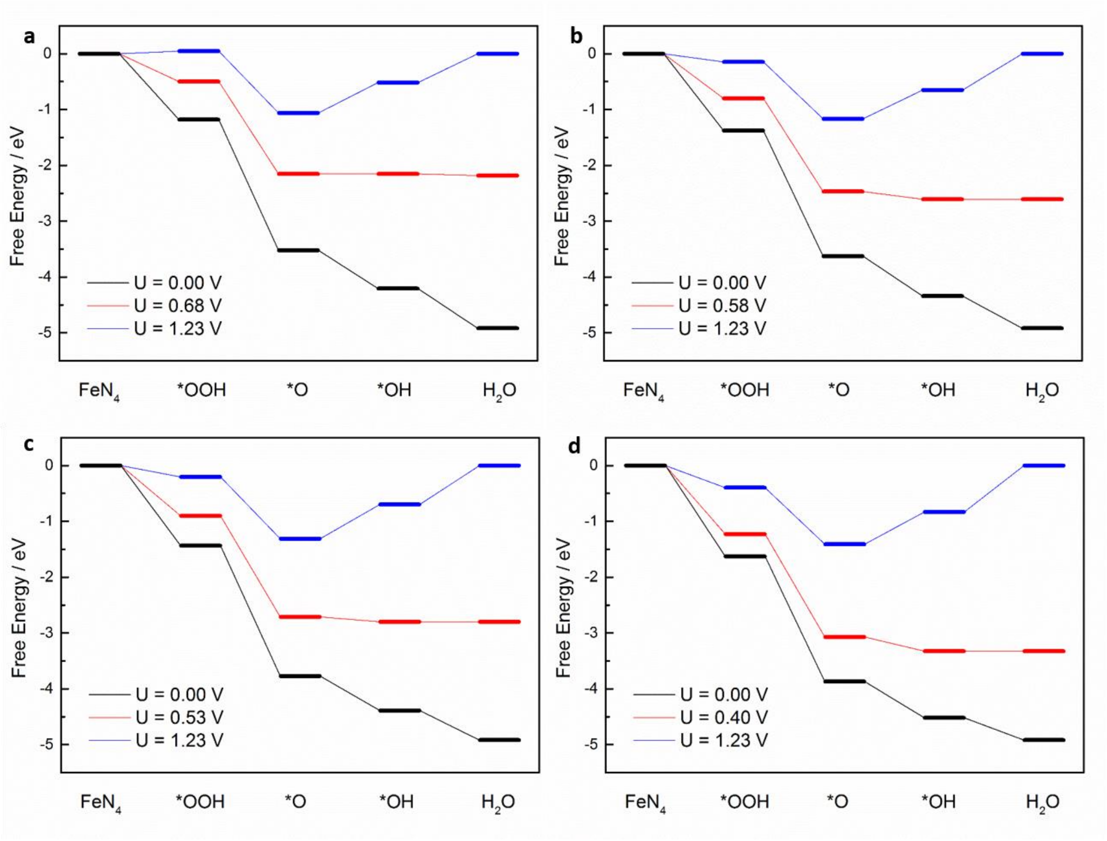

Fig. S3 Free energy diagrams of FeN_4 periodic model on ORR with different methods. The energy diagrams are based on the most stable spin state for each intermediate. (a) PBE, (b) PBE with Van der Waals interaction, (c) PBE in implicit solvent and (d) PBE with Van der Waals interaction in implicit solvent.

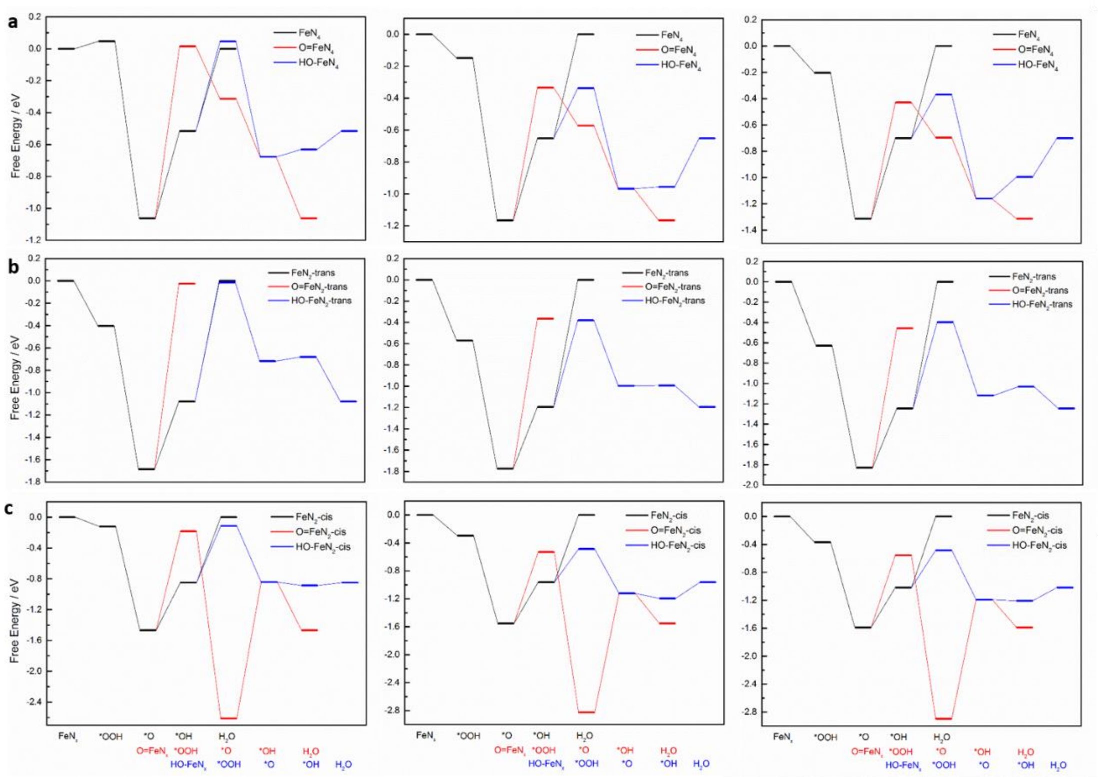

Fig. S4 Free energy diagrams for ORR assuming (a) FeN_4, (b) FeN_2-trans and (c) FeN_2-cis as active sites in PBE (left), with Van der Waals interaction included (middle) and in implicit solvent (right) in periodic models with CHE approach at equilibrium potential (1.23 V). Intermediate structures of $O=FeN_x$ or $HO\text{-}FeN_x$ (x=2 or 4) are also considered as active sites to start a second ORR cycle as shown with the red and blue lines and labels, respectively.

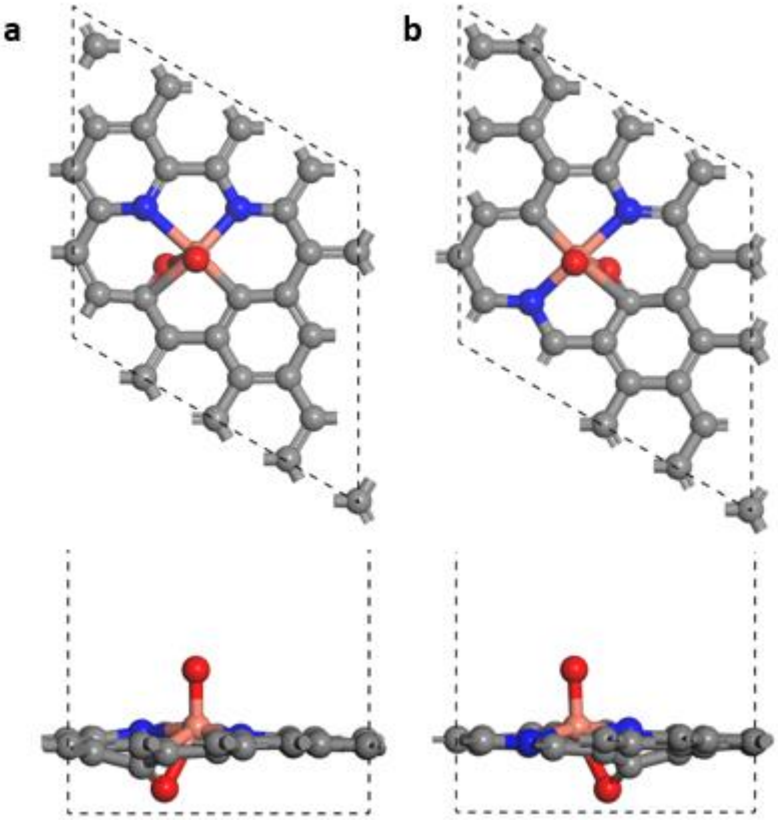

Fig. S5 The geometry of (a) O=FeN$_2$-cis-O and (b) O=FeN$_2$-trans-O from top view and side view. Grey, blue, orange, red and white spheres represent C, N, Fe, O and H atoms, respectively.

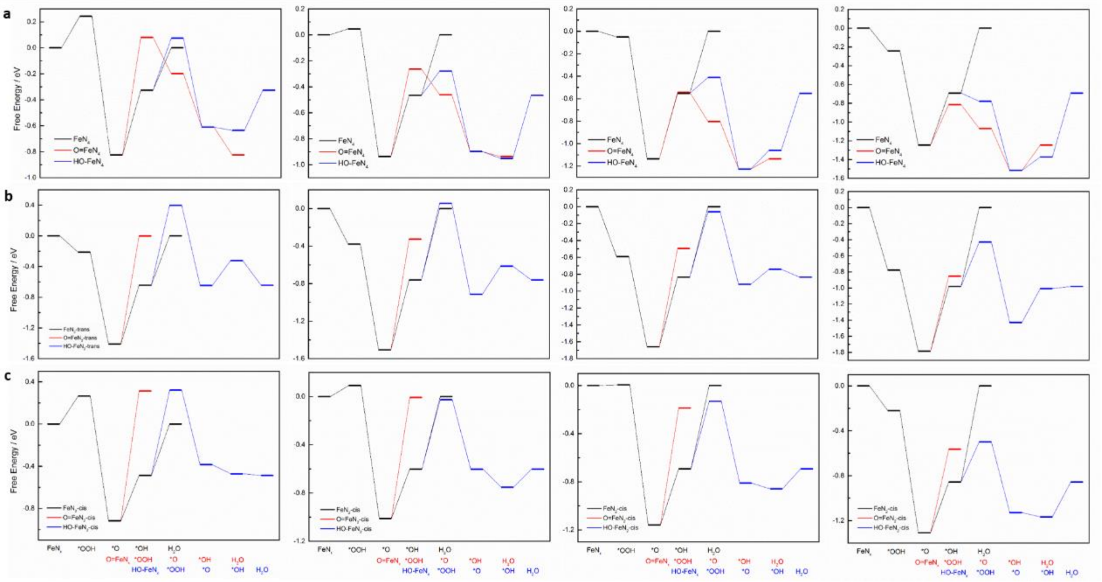

Fig. S6 Free energy diagrams for ORR assuming (a) FeN_4, (b) FeN_2-trans and (c) FeN_2-cis as active sites in PBE (left), in PBE, PBE with Van der Waals interaction, PBE in implicit solvent and PBE with Van der Waals interaction in implicit solvent (from left to right) in cluster models with CHE approach at equilibrium potential (1.23 V). Intermediate structures of O=FeN_x or HO-FeN_x (x=2 or 4) are also considered as active sites to start a second ORR cycle as shown with the red and blue lines and labels, respectively.

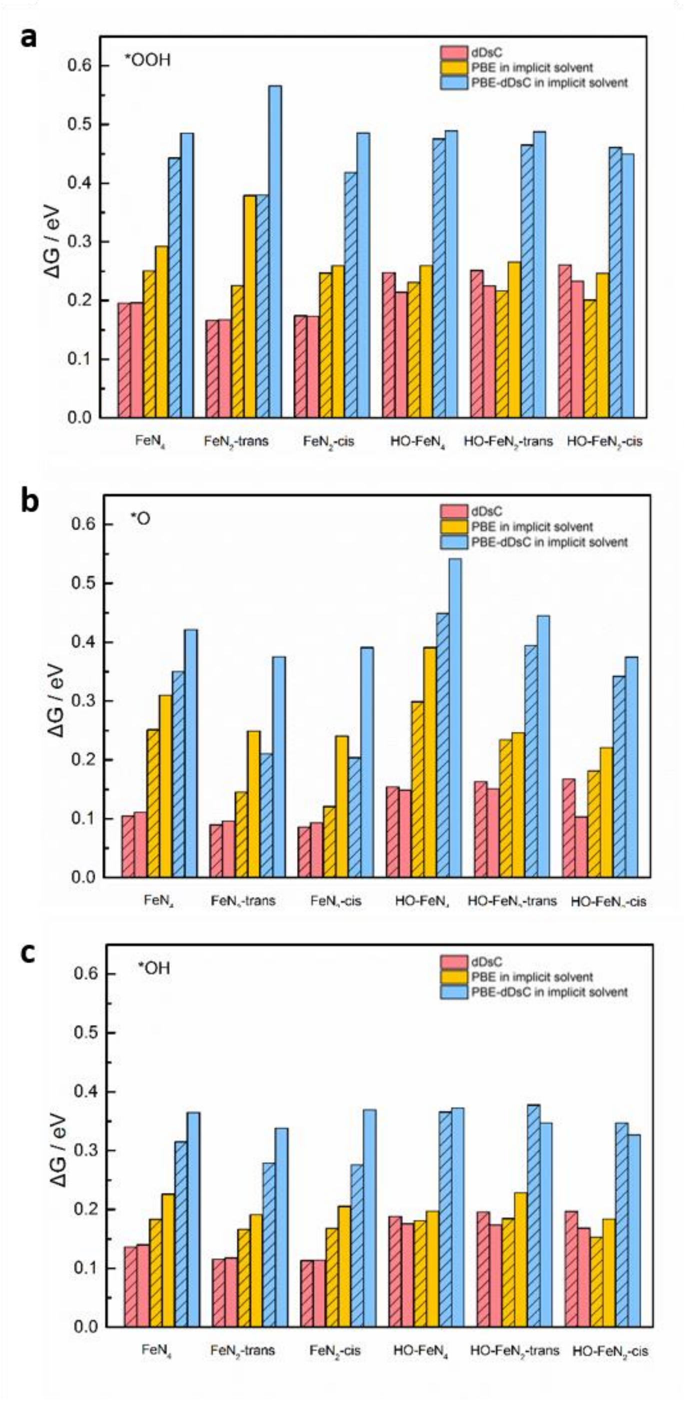

Fig. S7 The adsorption free energy difference of (a) OOH, (b) O and (c) OH on both periodic and cluster models with PBE results as the reference. The column bar in light red, orange and blue stands for results with Van der Waals interaction, implicit solvent and both effects included, respectively. The column bar in shadow and blank stands for the periodic and cluster models, respectively.

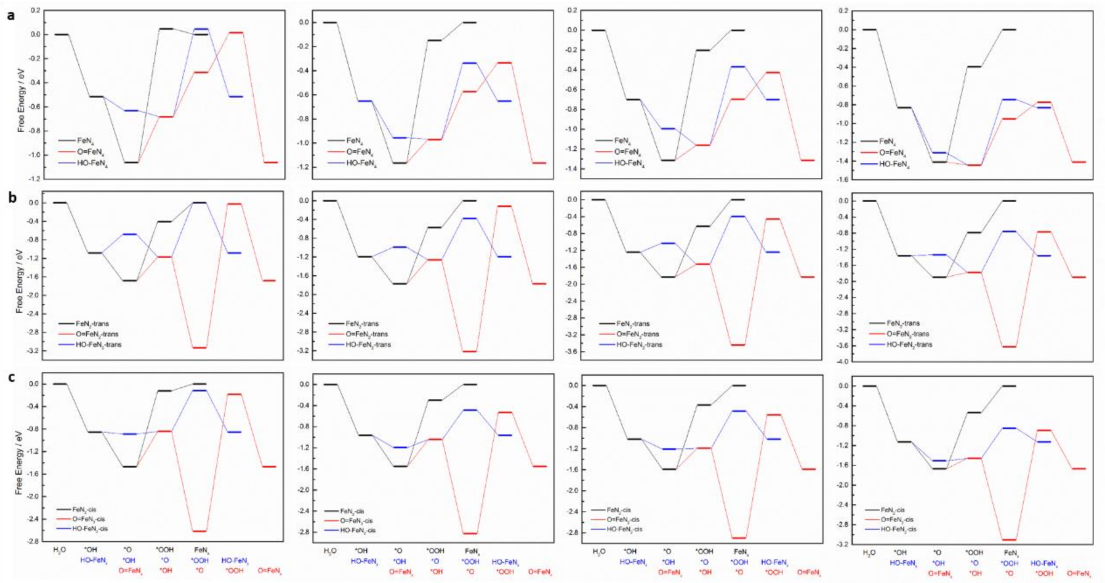

Fig. S8 Free energy diagrams for OER assuming (a) FeN_4, (b) FeN_2-trans and (c) FeN_2-cis as active sites in PBE, PBE with Van der Waals interaction, PBE in implicit solvent and PBE with Van der Waals interaction in implicit solvent (from left to right) in periodic models with CHE approach at equilibrium potential (1.23 V). Intermediate structures of HO-FeN_x or O=FeN_x (x=2 or 4) are also considered as active sites to start a second OER cycle as shown with the blue and red lines and labels, respectively.

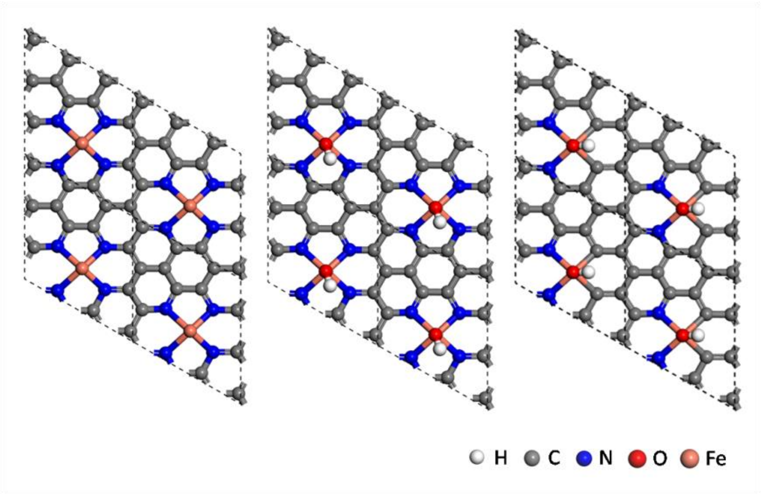

Fig. S9 The geometry for FeN_4, HO-FeN_4 and HO-FeN_2-cis. Grey, blue, orange, red and white spheres represent C, N, Fe, O and H atoms, respectively

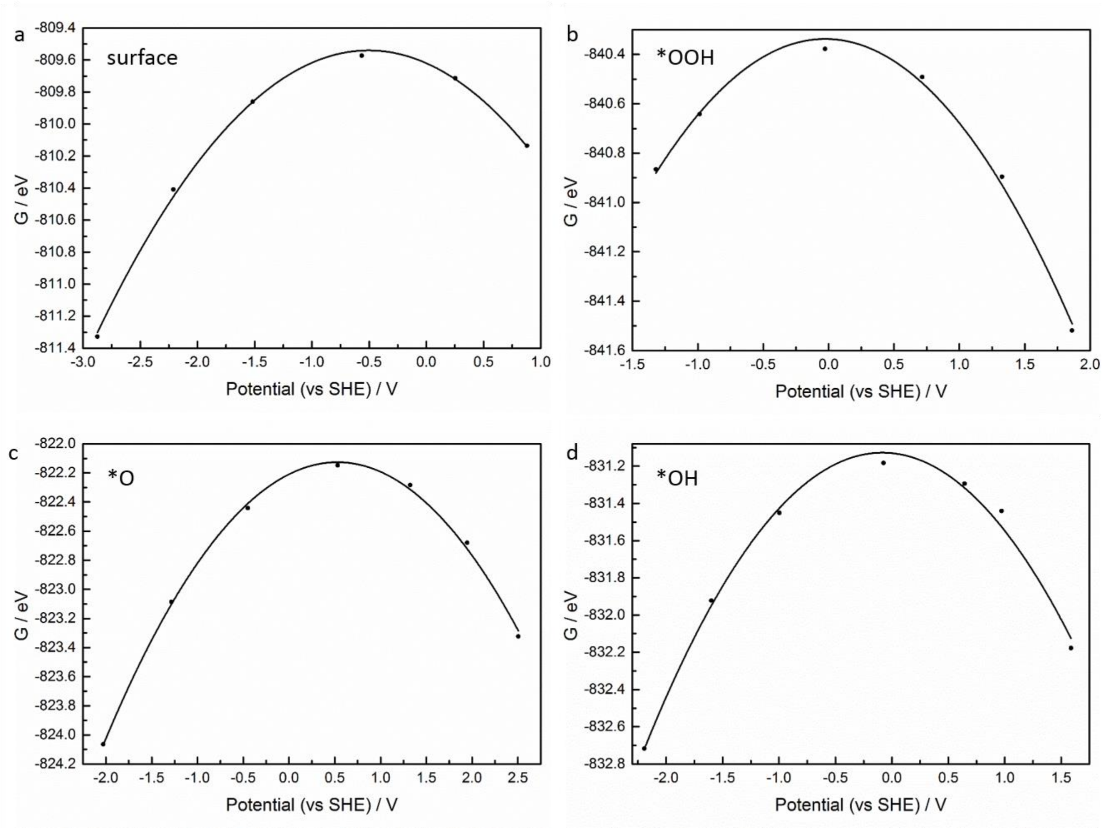

Fig. S10 The fitted G(V) parabola as a function of potential. (a) bare surface, (b) *OOH, (c) *O and (d) *OH on FeN_4.

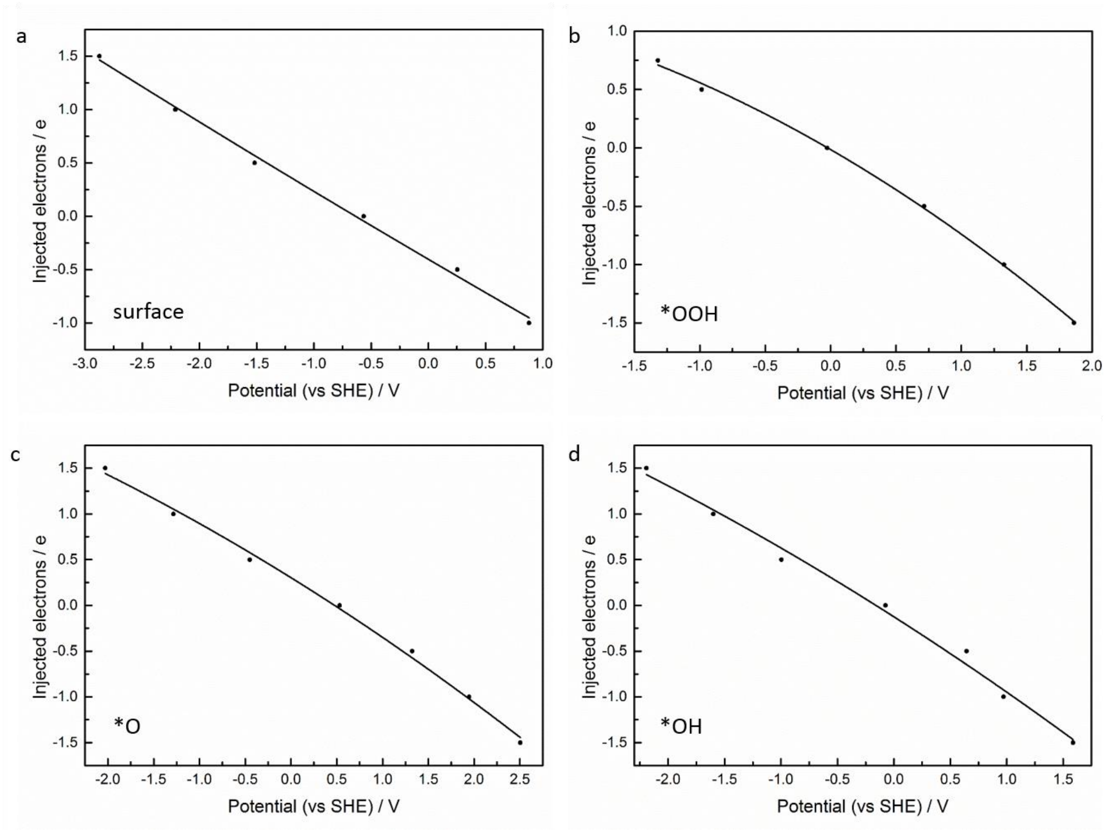

Fig. S11 The electronic charges as a function of potential. (a) bare surface, (b) *OOH, (c) *O and (d) *OH on FeN_4.

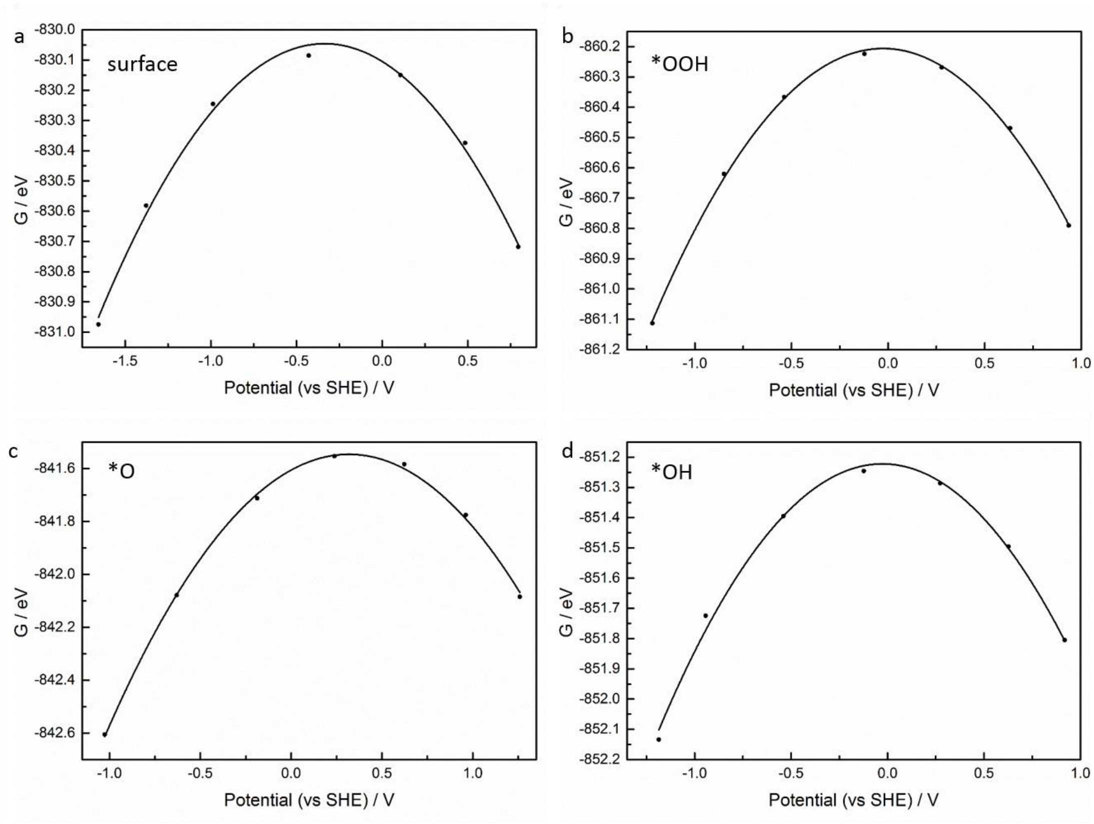

Fig. S12 The fitted G(V) parabola as a function of potential. (a) bare surface, (b) *OOH, (c) *O and (d) *OH on HO-FeN$_4$.

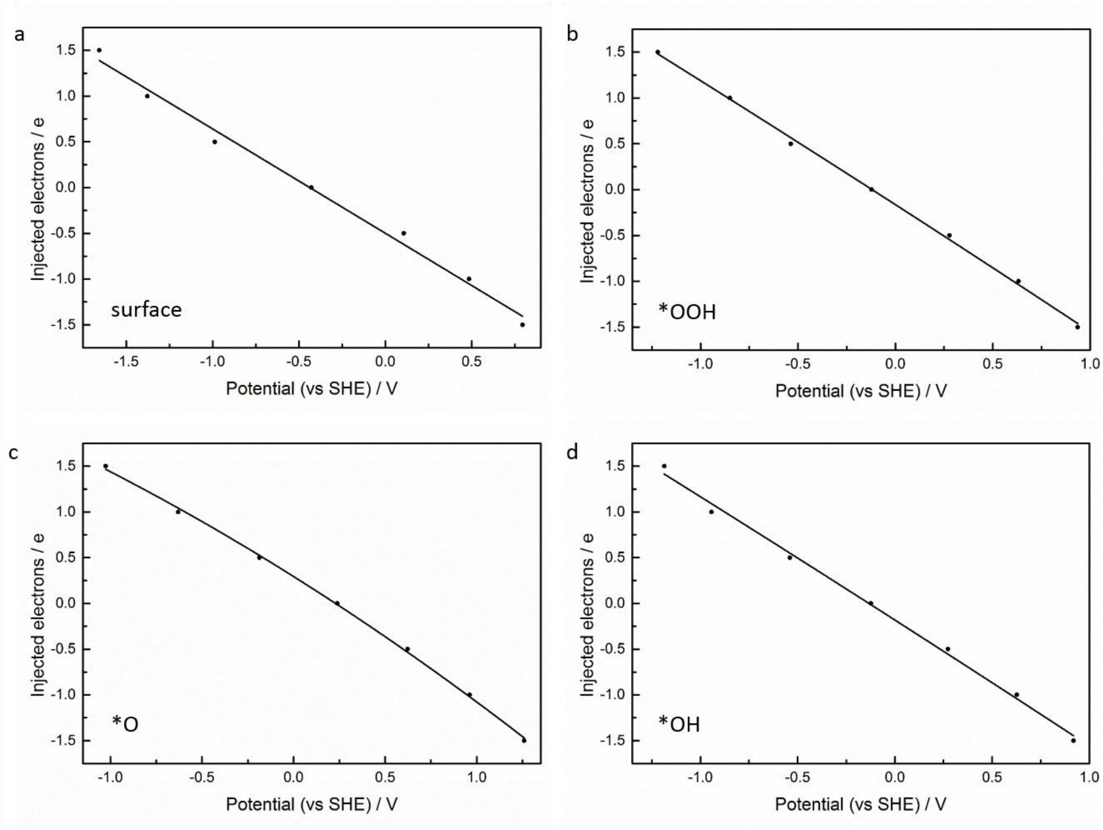

Fig. S13 The electronic charges as a function of potential. (a) bare surface, (b) *OOH, (c) *O and (d) *OH on HO-FeN_4.

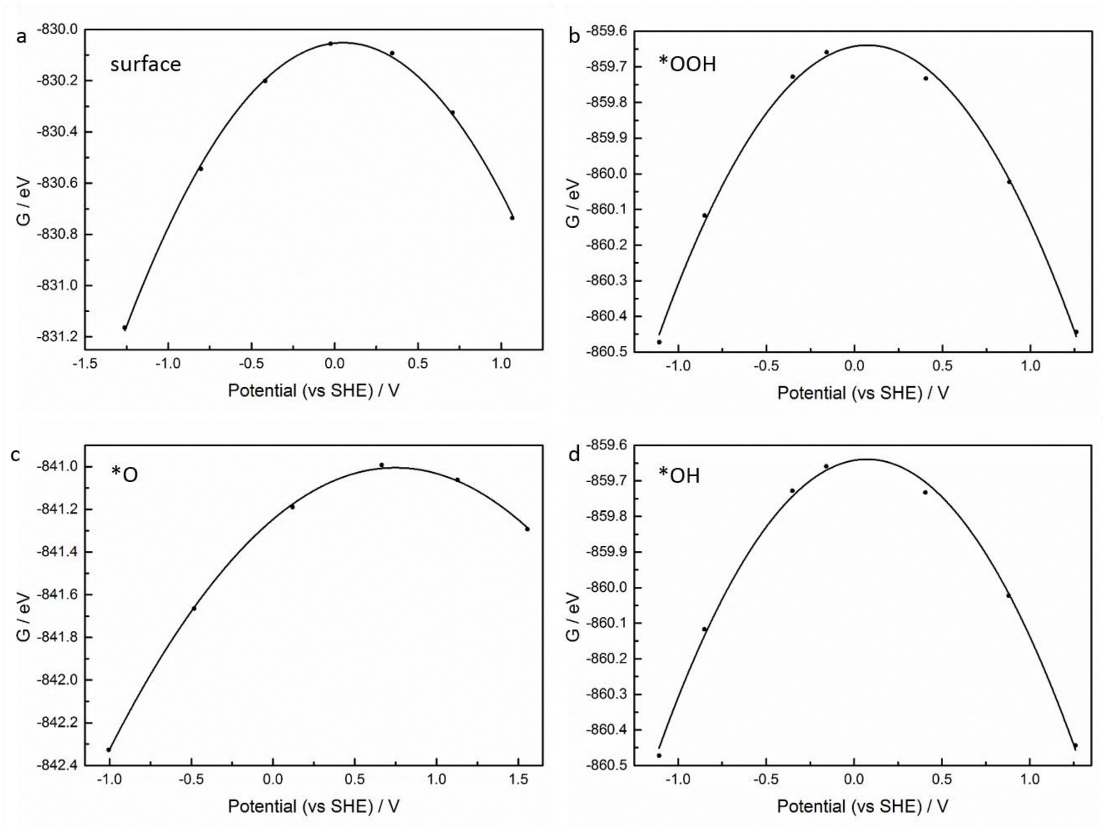

Fig. S14 The fitted G(V) parabola as a function of potential. (a) bare surface, (b) *OOH, (c) *O and (d) *OH on HO-FeN_2-cis.

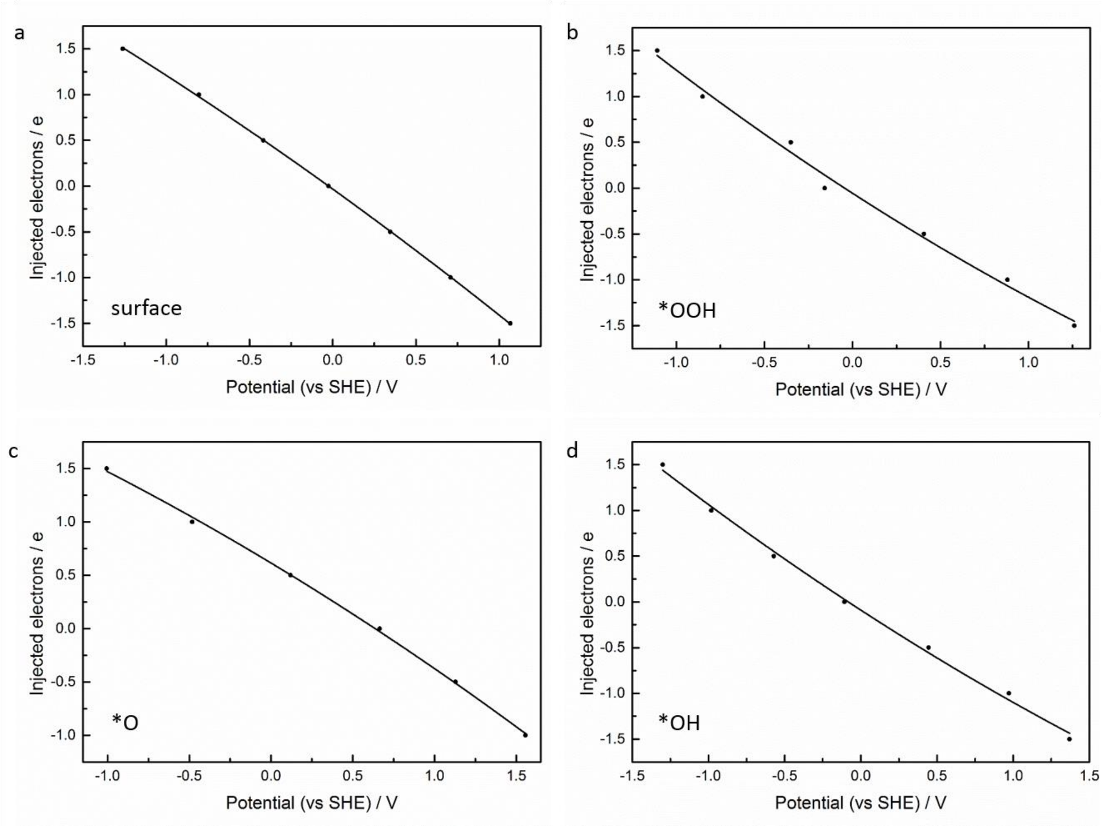

Fig. S15 The electronic charges as a function of potential. (a) bare surface, (b) *OOH, (c) *O and (d) *OH on HO-FeN$_2$-cis.

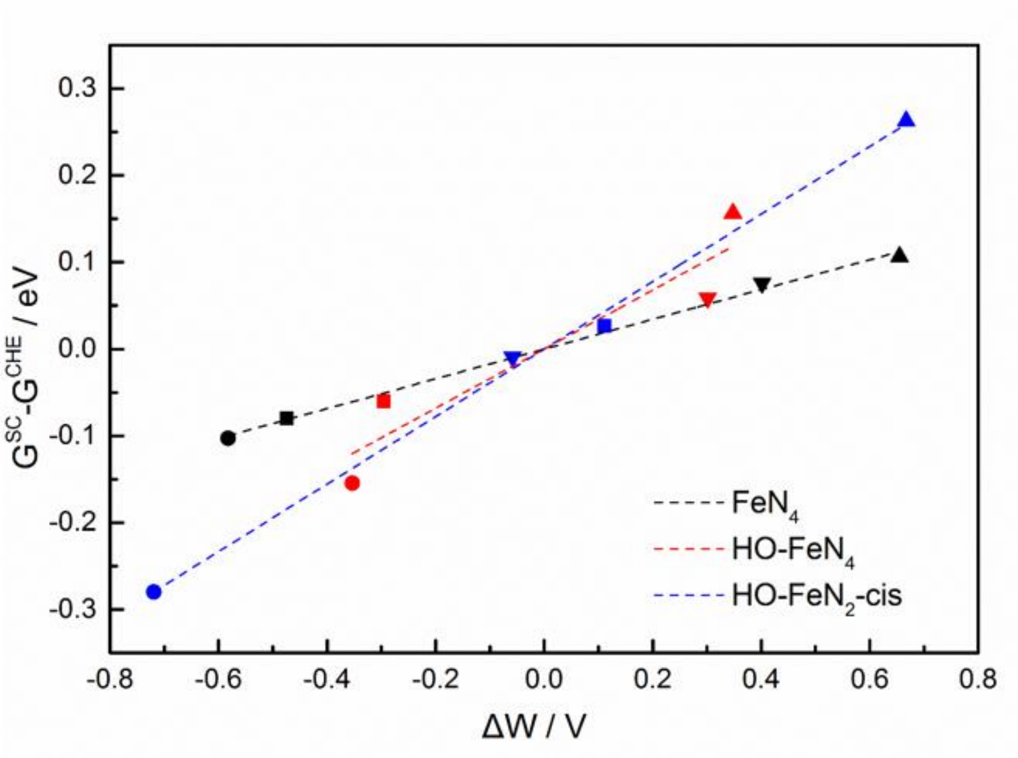

Fig. S16 The difference in free energy of elementary steps between SC and CHE approaches on FeN_4 (black), HO-FeN_4 (red) and HO-FeN_2-cis (blue) as a function of difference in workfunction at 0.0 charge. Four elementary steps in ORR are shown by square, circle, triangle and inverted triangle in sequence. The energy for SC is chosen at the 0.0 V and which is chosen at 0.0 charge for CHE.

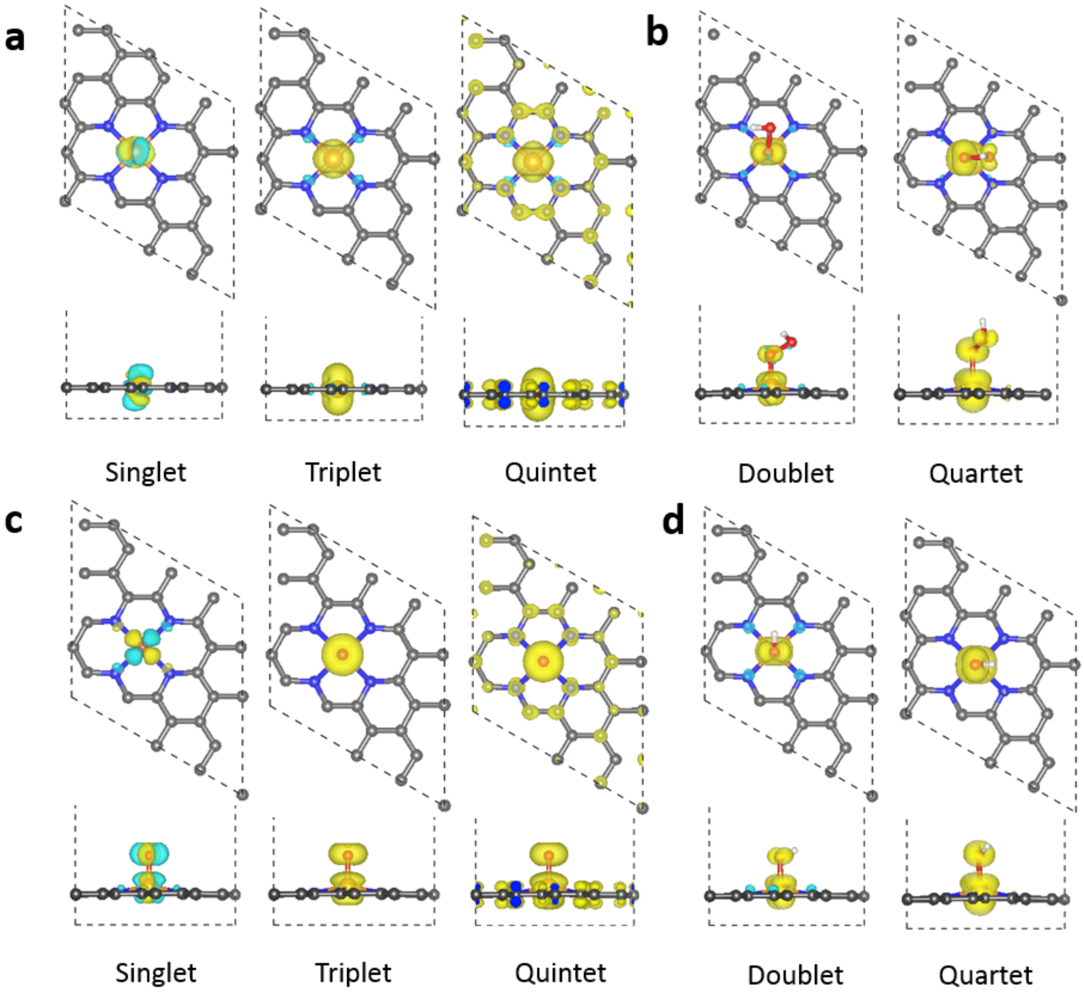

Fig. S17 Top view and side view of spin density on (a) bare FeN_4 active site (b) *OOH (c) *O and (d) *OH in periodic models at isosurface level 0.005, where light blue represents negative and yellow represents positive spin density. Different spin states were considered for the bare site and intermediates. Grey, blue, orange, red and white spheres represent C, N, Fe, O and H atoms, respectively.

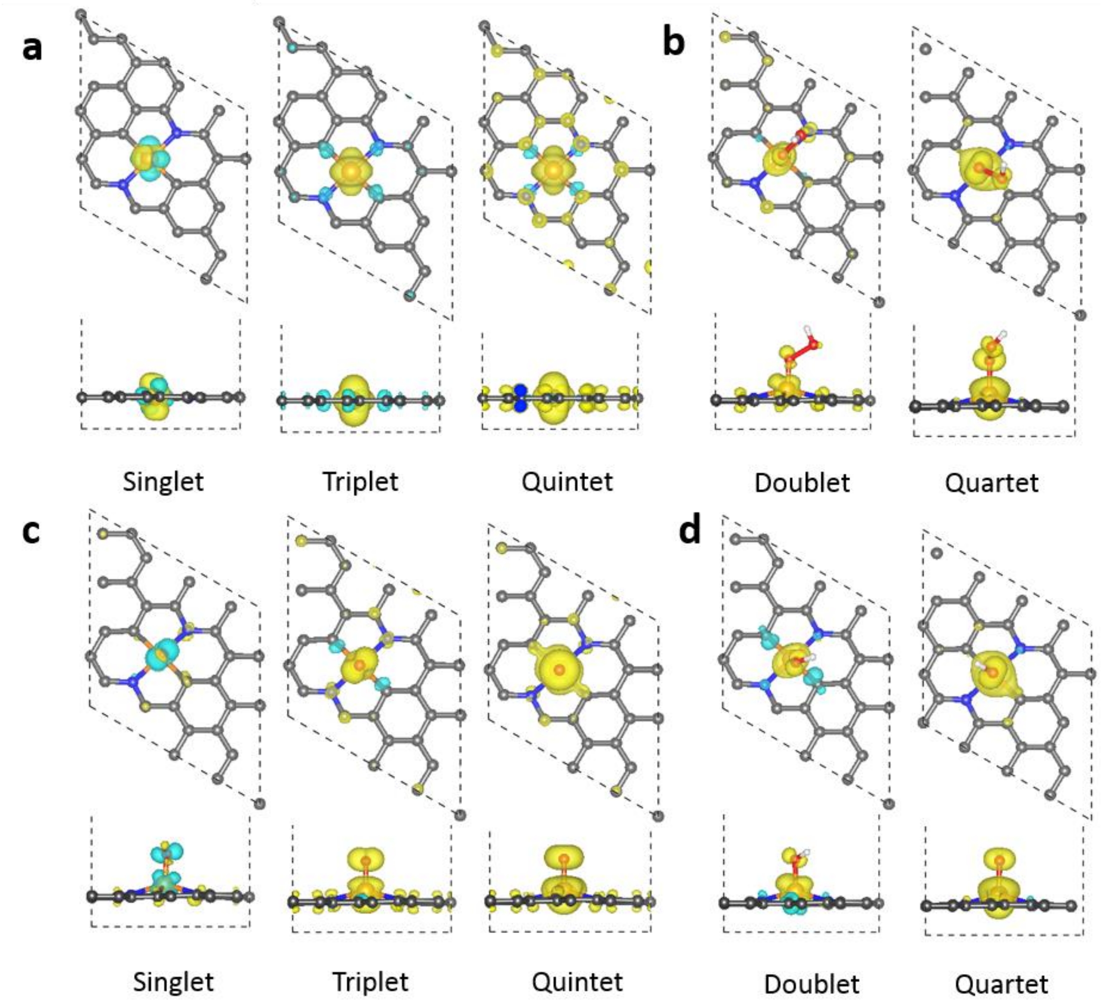

Fig. S18 Top view and side view of spin density on (a) bare FeN_2–trans active site (b) *OOH (c) *O and (d) *OH in periodic models at isosurface level 0.005, where light blue represents negative and yellow represents positive spin density. Different spin states were considered for the bare site and intermediates. Grey, blue, orange, red and white spheres represent C, N, Fe, O and H atoms, respectively.

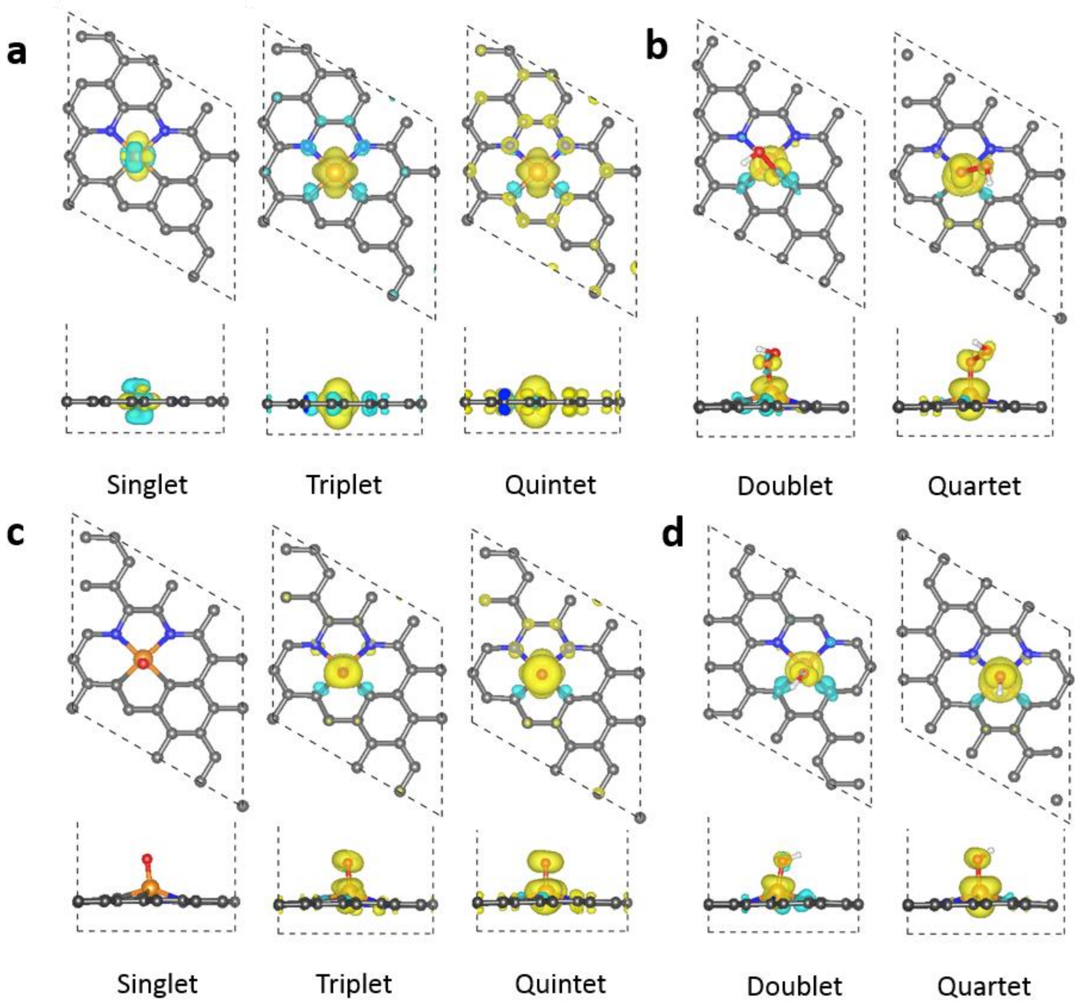

Fig. S19 Top view and side view of spin density on (a) bare FeN_2-cis active site (b) *OOH (c) *O and (d) *OH in periodic models at isosurface level 0.005, where light blue represents negative and yellow represents positive spin density. Different spin states were considered for the bare site and intermediates. Grey, blue, orange, red and white spheres represent C, N, Fe, O and H atoms, respectively.

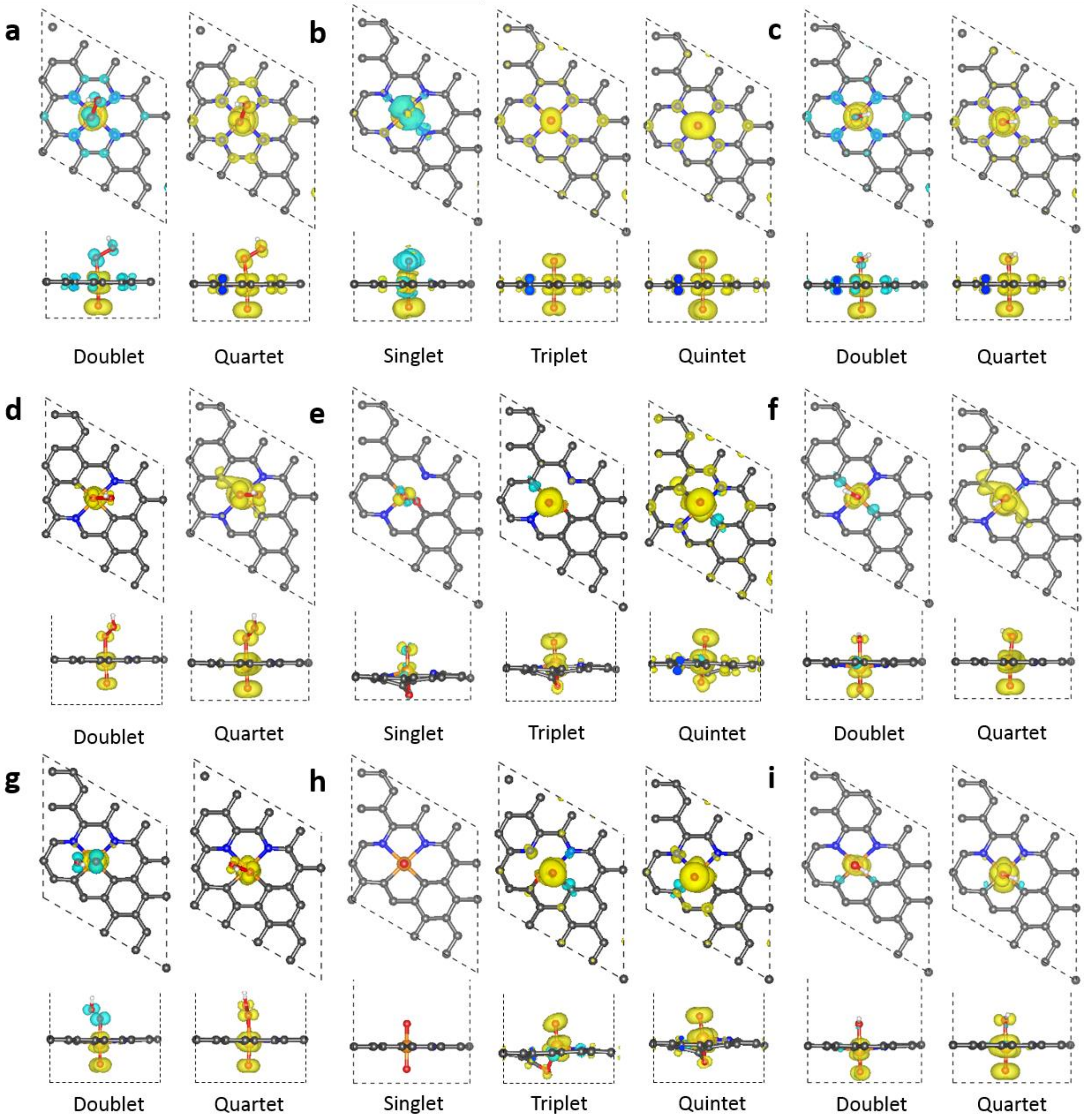

Fig. S20 Top view and side view of spin density on (a) *OOH (b) *O (c) *OH of O=FeN$_4$ active sites, (d) *OOH (e) *O (f) *OH of O=FeN$_2$-trans active sites and (g) *OOH (h) *O (i) *OH of O=FeN$_2$-cis active sites in periodic models at isosurface level 0.005, where light blue represents negative and yellow represents positive spin density. Different spin states were considered for the bare site and intermediates. Grey, blue, orange, red and white spheres represent C, N, Fe, O and H atoms, respectively.

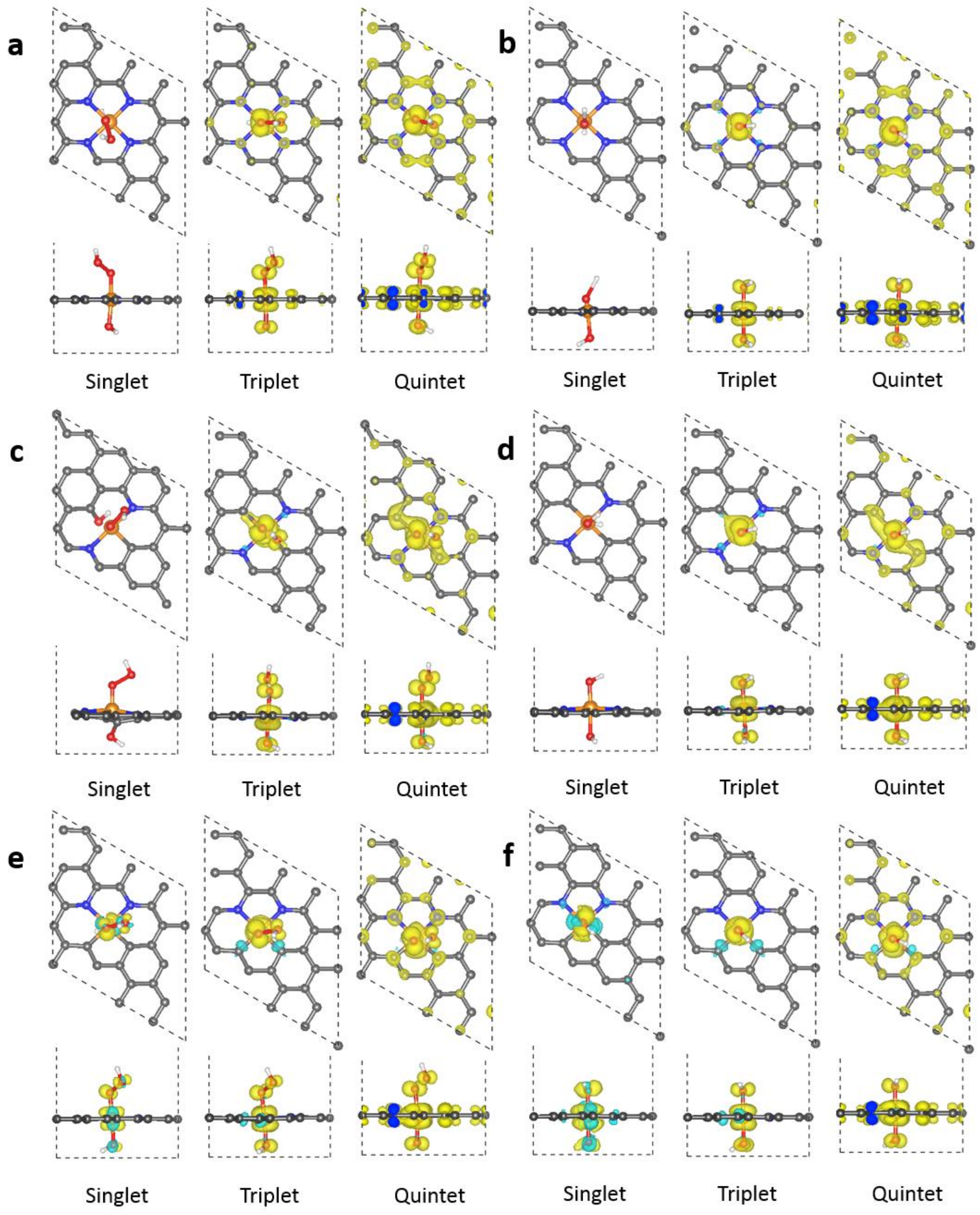

Fig. S21 Top view and side view of spin density on (a) *OOH (b) *OH of HO-FeN$_4$ active sites, (c) *OOH (d) *OH of HO-FeN$_2$-trans active sites and (e) *OOH (f) *OH of HO-FeN$_2$-cis active site in periodic models at isosurface level 0.005, where light blue represents negative and yellow represents positive spin density. Different spin states were considered for the bare sites and intermediates. Grey, blue, orange, red and white spheres represent C, N, Fe, O and H atoms, respectively.

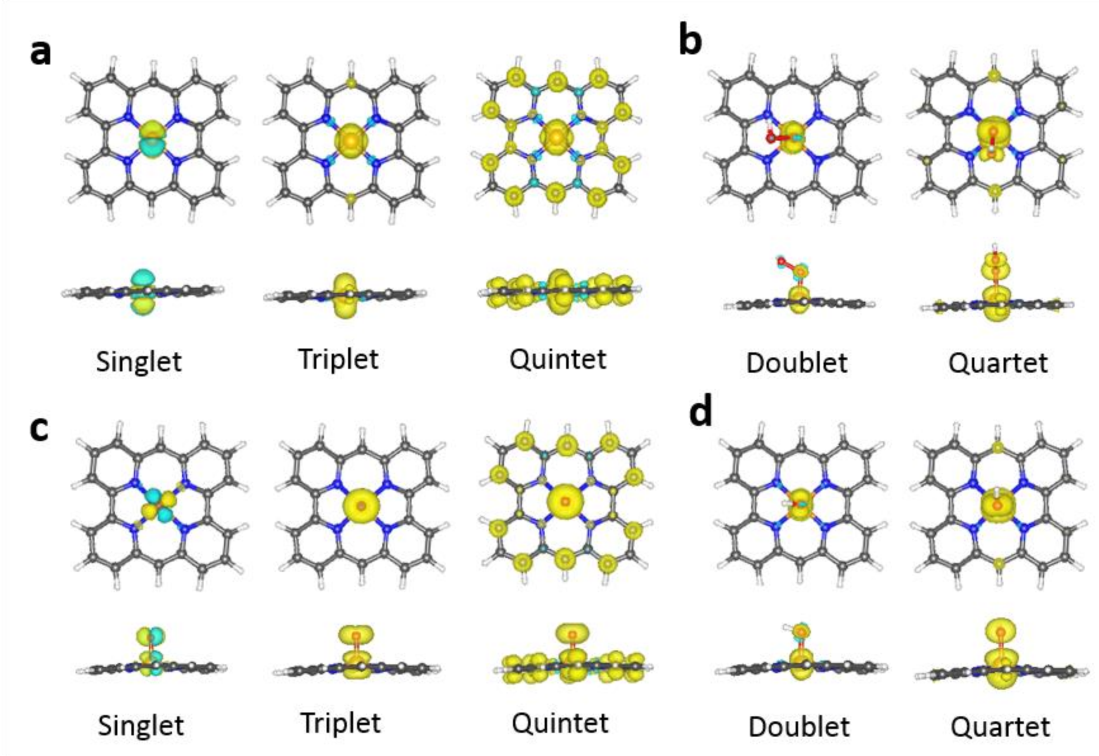

Fig. S22 Top view and side view of spin density on (a) bare FeN_4 active site (b) *OOH (c) *O and (d) *OH in cluster models at isosurface level 0.005, where light blue represents negative and yellow represents positive spin density. Different spin states were considered for the bare site and intermediates. Grey, blue, orange, red and white spheres represent C, N, Fe, O and H atoms, respectively.

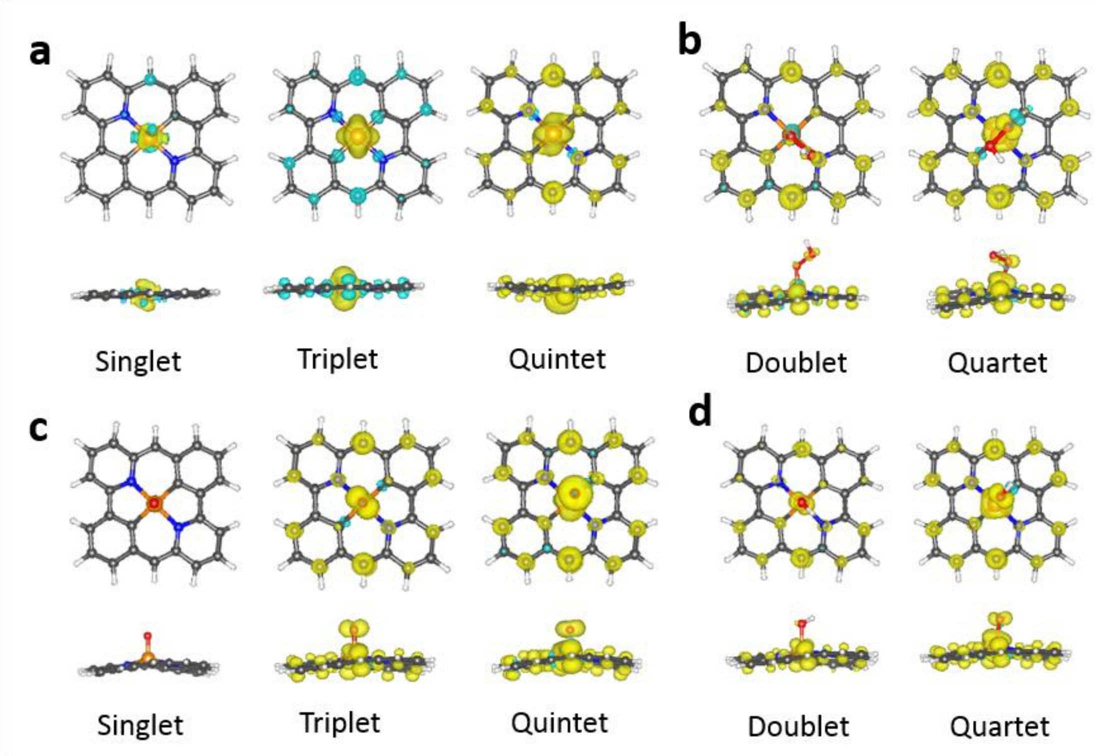

Fig. S23 Top view and side view of spin density on (a) bare FeN_2–trans active site (b) *OOH (c) *O and (d) *OH in cluster models at isosurface level 0.005, where light blue represents negative and yellow represents positive spin density. Different spin states were considered for the bare site and intermediates. Grey, blue, orange, red and white spheres represent C, N, Fe, O and H atoms, respectively.

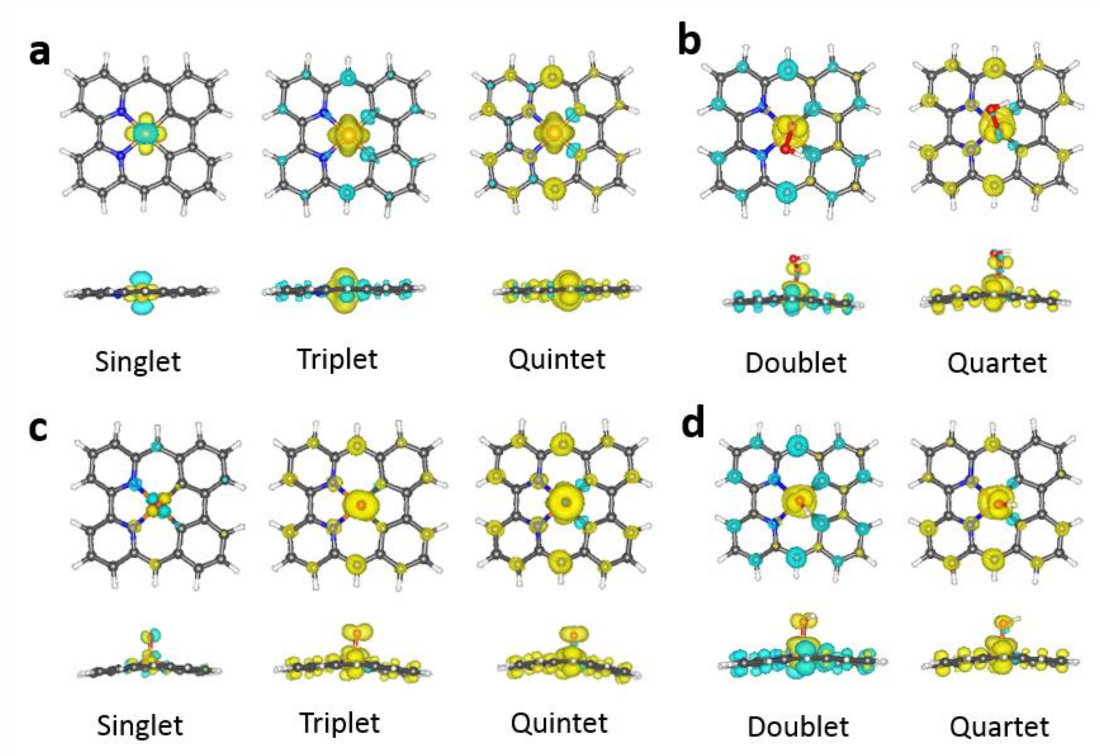

Fig. S24 Top view and side view of spin density on (a) bare FeN_2-cis active site (b) *OOH (c) *O and (d) *OH in cluster models at isosurface level 0.005, where light blue represents negative and yellow represents positive spin density. Different spin states were considered for the bare site and intermediates. Grey, blue, orange, red and white spheres represent C, N, Fe, O and H atoms, respectively.

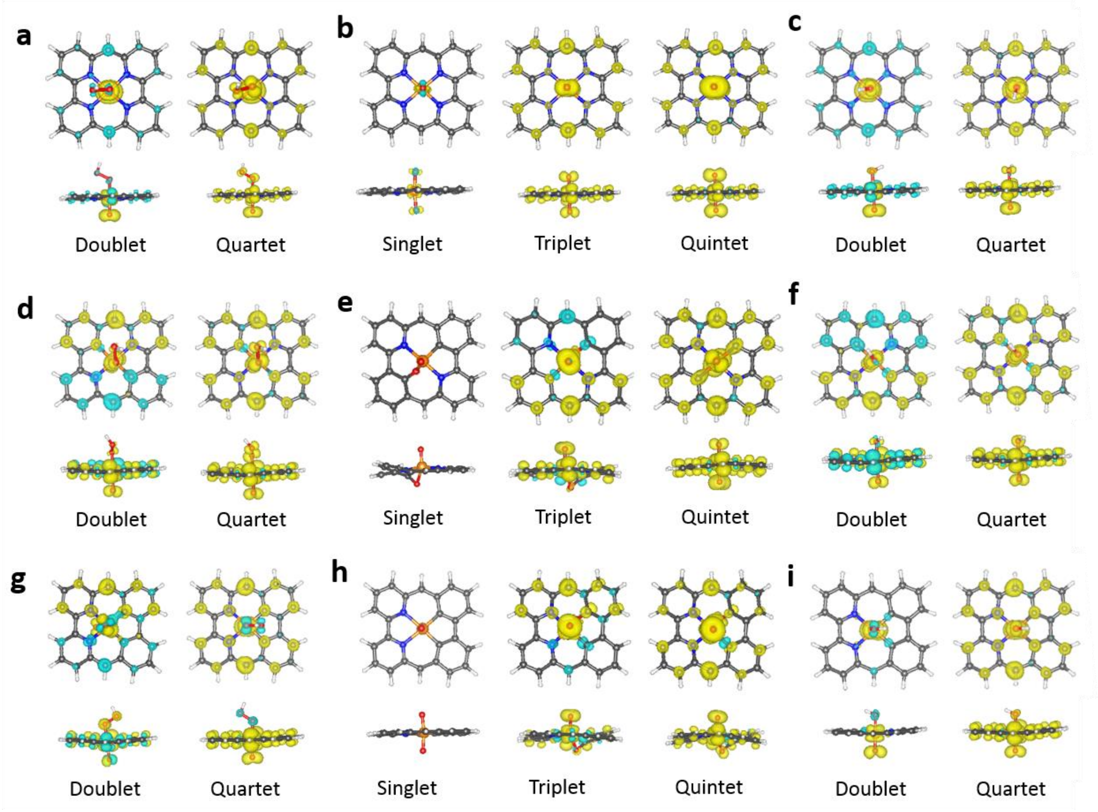

Fig. S25 Top view and side view of spin density on (a) *OOH (b) *O (c) *OH of O=FeN$_4$ active sites, (d) *OOH (e) *O (f) *OH of O=FeN$_2$-trans active sites and (g) *OOH (h) *O (i) *OH of O=FeN$_2$-cis active sites in cluster models at isosurface level 0.005, where light blue represents negative and yellow represents positive spin density. Different spin states were considered for the bare site and intermediates. Grey, blue, orange, red and white spheres represent C, N, Fe, O and H atoms, respectively.

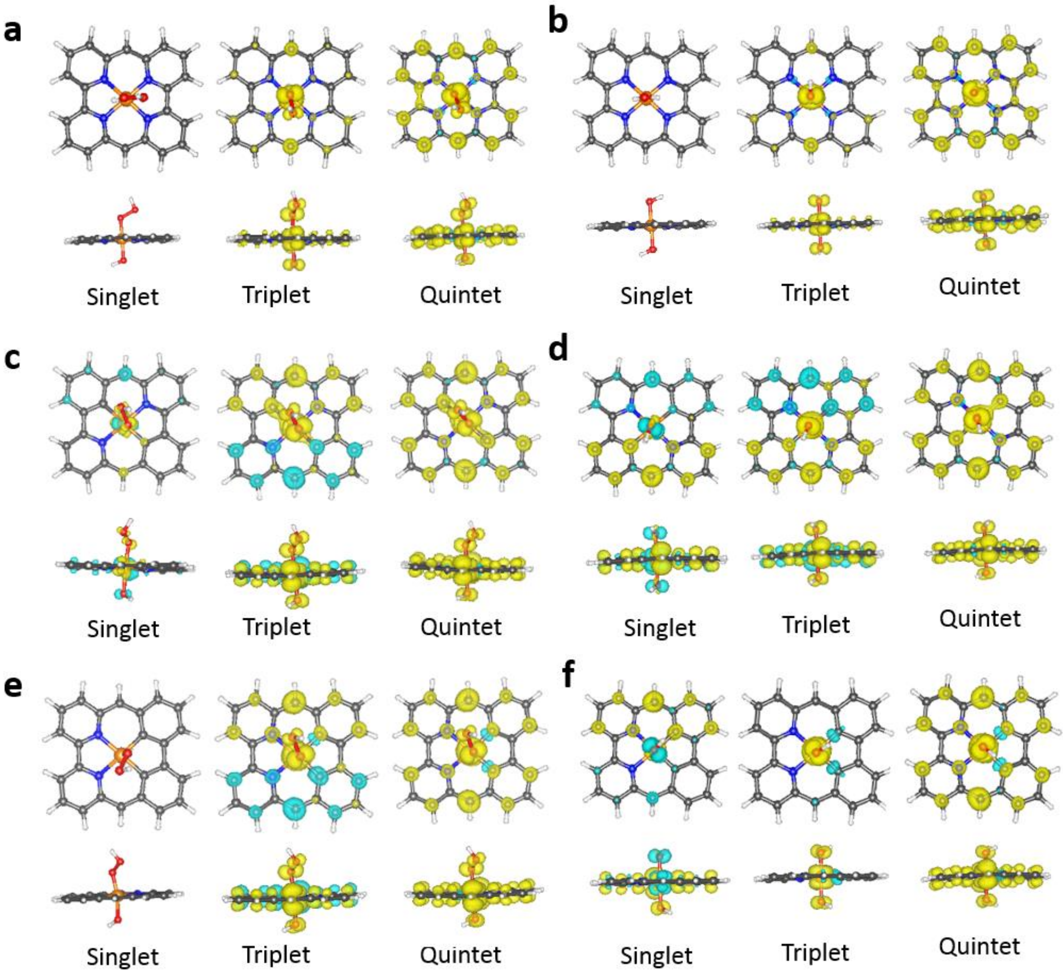

Fig. S26 Top view and side view of spin density on (a) *OOH (b) *OH of HO-FeN$_4$ active sites, (c) *OOH (d) *OH of HO-FeN$_2$-trans active sites and (e) *OOH (f) *OH of HO-FeN$_2$-cis active site in cluster models at isosurface level 0.005, where light blue represents negative and yellow represents positive spin density. Different spin states were considered for the bare sites and intermediates. Grey, blue, orange, red and white spheres represent C, N, Fe, O and H atoms, respectively.

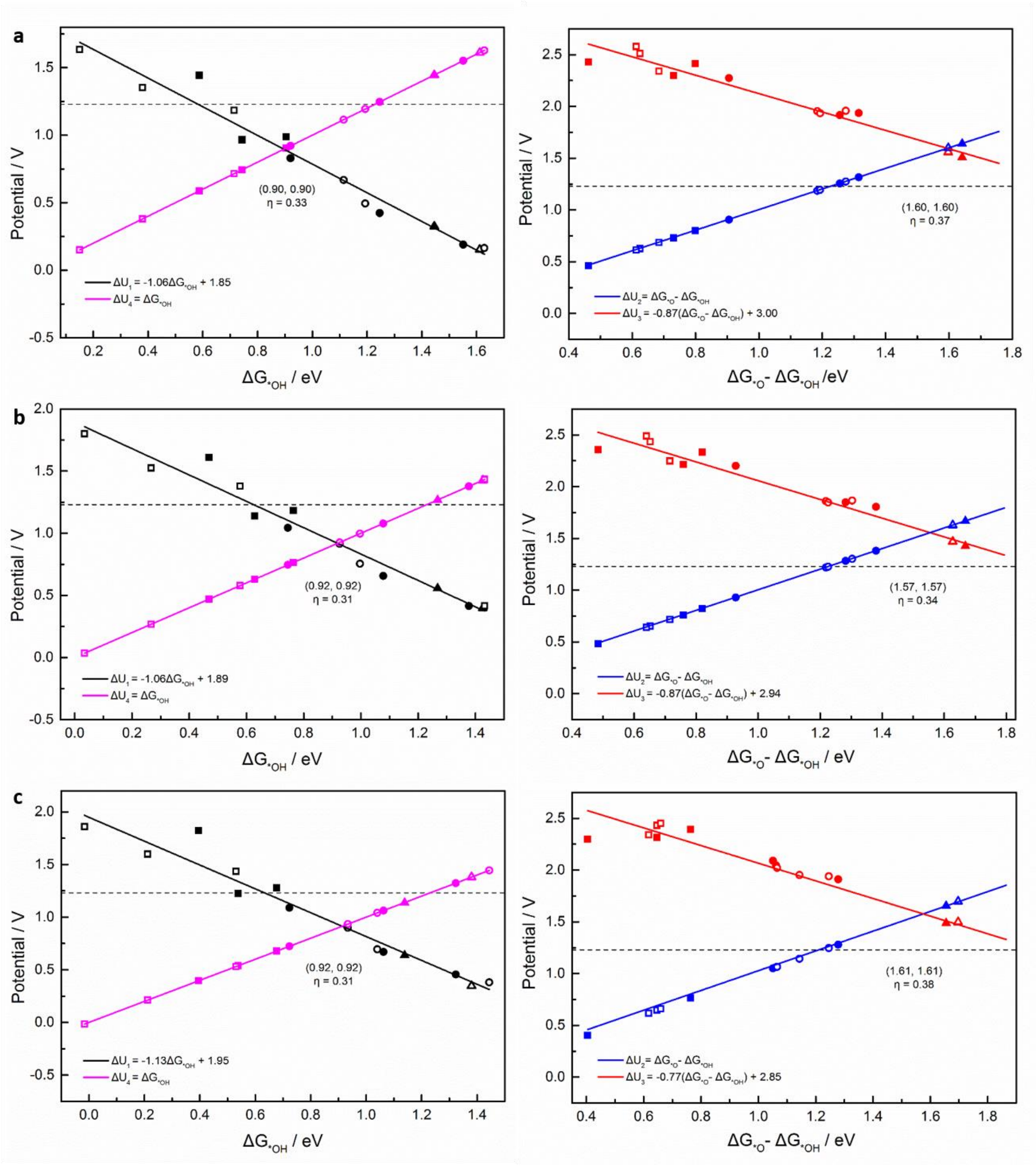

Fig. S27 Potential scaling relations as a function of OH adsorption free energy for ORR (left) and potential scaling relations as a function of the difference between O and OH adsorption free energy for OER (right) with different methods applied. The energies are based on the most stable spin state of each intermediate for periodic (empty symbols) and cluster (solid symbols) models. The square, the circle and the triangle symbols stand for the FeN_x, HO-FeN_x (x=2 or 4) and O=FeN_4, respectively. (a) PBE, (b) PBE with Van der Waals interaction and (c) PBE in implicit solvent.

Table S1 Data of free energies of steps on periodic models.

	Product (step)	Free energy / eV			
		PBE	PBE-dDsC	PBE in implicit solvent	PBE-dDsC in implicit solvent
FeN$_4$-OH	**FeN$_4$** (G_4)	-0.71	-0.58	-0.53	-0.40
	HO-FeN$_4$-OOH (G_1)	-0.67	-0.92	-0.90	-1.14
FeN$_4$-O	**FeN$_4$**-OH (G_3)	-0.68	-0.72	-0.62	-0.65
	O=FeN$_4$-OOH (G_1)	-0.15	-0.40	-0.35	-0.60
FeN$_2$-trans-OH	**FeN$_2$-trans** (G_4)	-0.15	-0.03	0.02	0.13
	HO-FeN$_2$-trans-OOH (G_1)	-0.16	-0.42	-0.38	-0.63
FeN$_2$-trans-O	**FeN$_2$-trans**-OH (G_3)	-0.63	-0.65	-0.65	-0.69
	O=FeN$_2$-trans-OOH (G_1)	0.43	0.18	0.14	-0.10
FeN$_2$-cis-OH	**FeN$_2$-cis** (G_4)	-0.38	-0.27	-0.21	-0.10
	HO-FeN$_2$-cis-OOH (G_1)	-0.49	-0.75	-0.69	-0.95
FeN$_2$-cis-O	**FeN$_2$-cis**-OH (G_3)	-0.61	-0.64	-0.66	-0.68
	O=FeN$_2$-cis-OOH (G_1)	0.05	-0.21	-0.20	-0.46

Table S2 Data of free energies of steps on cluster models.

	Product (step)	Free energy / eV			
		PBE	PBE-dDsC	PBE in implicit solvent	PBE-dDsC in implicit solvent
FeN$_4$-OH	**FeN$_4$** (G_4)	-0.90	-0.76	-0.68	-0.54
	HO-FeN$_4$-OOH (G_1)	-0.83	-1.04	-1.09	-1.32
FeN$_4$-O	**FeN$_4$**-OH (G_3)	-0.73	-0.76	-0.65	-0.67
	O=FeN$_4$-OOH (G_1)	-0.32	-0.56	-0.64	-0.80
FeN$_2$-trans-OH	**FeN$_2$-trans** (G_4)	-0.59	-0.47	-0.40	-0.25
	HO-FeN$_2$-trans-OOH (G_1)	-0.19	-0.41	-0.46	-0.68
FeN$_2$-trans-O	**FeN$_2$-trans**-OH (G_3)	-0.46	-0.48	-0.40	-0.42
	O=FeN$_2$-trans-OOH (G_1)	0.18	-0.05	-0.06	-0.30
FeN$_2$-cis-OH	**FeN$_2$-cis** (G_4)	-0.74	-0.63	-0.54	-0.37
	HO-FeN$_2$-cis-OOH (G_1)	-0.42	-0.66	-0.67	-0.87
FeN$_2$-cis-O	**FeN$_2$-cis**-OH (G_3)	-0.80	-0.82	-0.76	-0.78
	O=FeN$_2$-cis-OOH (G_1)	0.00	-0.23	-0.26	-0.49

Table S3 Parabolas of intermediates in symmetric systems.

Intermediates	FeN_4	HO-FeN_4	HO-FeN_2-cis
Surface	$y = -0.31x^2-0.28x-809.47$	$y = -0.52x^2-0.35x-830.10$	$y = -0.65x^2+0.07x-830.05$
*OOH	$y = -0.33x^2-0.02x-840.34$	$y = -0.63x^2-0.03x-860.21$	$y = -0.58x^2+0.09x-859.64$
*O	$y = -0.30x^2+0.31x-822.21$	$y = -0.59x^2+0.38x-841.61$	$y = -0.43x^2+0.65x-841.25$
*OH	$y = -0.35x^2-0.06x-831.14$	$y = -0.65x^2-0.03x-851.22$	$y = -0.50x^2+0.05x-850.94$

Table S4 Parabolas of steps in symmetric systems.

Steps	FeN_4	HO-FeN_4	HO-FeN_2-cis
ΔG_1	$y = -0.01x^2+0.13x-1.61$	$y = -0.05x^2+0.16x-1.20$	$y = 0.04x^2+0.01x-0.89$
ΔG_2	$y = 0.01x^2+0.17x-2.17$	$y = 0.02x^2+0.20x-1.96$	$y = 0.07x^2+0.28-2.07$
ΔG_3	$y = -0.03x^2-0.19x-0.74$	$y = -0.03x^2-0.21x-1.06$	$y = -0.03x^2-0.30x-1.09$
ΔG_4	$y = 0.02x^2-0.11x-0.39$	$y = 0.07x^2-0.16x-0.70$	$y = -0.08x^2+0.01x-0.87$

Table S5 Overpotential of different active sites for ORR and OER with CHE and SC approaches.

	Overpotential / V	FeN_4	HO-FeN_4	HO-FeN_2-cis
ORR	CHE	0.81	0.53	0.37
	SC	0.79	0.45	0.38
OER	CHE	0.89	0.69	0.65
	SC	0.59	0.35	0.47

Table S6 Magnetic moment of Fe and O in FeN$_x$ and their intermediates in periodic models

Magnetic moment /μ_B	Bare active site			*OOH		*O			*OH	
	Singlet	Triplet	Quintet	Doublet	Quartet	Singlet	Triplet	Quintet	Doublet	Quartet
μ_{Fe} [a]	-0.08	1.91	2.12	0.98	2.20	0.01	1.24	1.66	1.07	2.31
μ_{O} [a]	-	-	-	0.12	0.33	0.00	0.57	0.63	0.11	0.28
μ_{Fe} [b]	0.23	2.36	2.67	0.54	2.24	-0.28	0.94	2.41	1.21	2.39
μ_{O} [b]	-	-	-	0.04	0.21	-0.01	0.31	0.66	0.06	0.20
μ_{Fe} [c]	0.17	2.47	2.66	1.18	2.28	0.00	1.11	2.40	1.31	2.44
μ_{O} [c]	-	-	-	0.06	0.18	0.00	0.30	0.61	0.07	0.18

[a] FeN$_4$. [b] FeN$_2$-trans. [c] FeN$_2$-cis.

Table S7 Magnetic moment of Fe and O in O=FeN$_x$ and their intermediates in periodic models

Magnetic moment /μ_B	Bare active site			*OOH		*O			*OH	
	Singlet	Triplet	Quintet	Doublet	Quartet	Singlet	Triplet	Quintet	Doublet	Quartet
μ_{Fe} [a]	0.01	1.24	1.66	1.00	1.13	0.62	0.51	1.13	1.04	1.19
$\mu_{O\,(\mathbf{O}=Fe)}$ [a]	0.00	0.57	0.63	0.59	0.65	0.50	0.20	0.79	0.55	0.65
μ_{O} [a]	-	-	-	-0.12	0.17	-0.34	0.21	0.74	0.00	0.09
μ_{Fe} [b]	-0.28	0.94	2.41	0.81	1.52	0.06	1.20	1.99	0.70	1.64
$\mu_{O\,(\mathbf{O}=Fe)}$ [b]	-0.01	0.31	0.66	0.33	0.63	-0.02	0.03	0.09	0.26	0.68
μ_{O} [b]	-	-	-	-0.01	0.21	0.06	0.46	0.56	0.03	0.15
μ_{Fe} [c]	0.00	1.11	2.40	0.71	1.77	0.00	1.20	2.59	0.73	1.98
$\mu_{O\,(\mathbf{O}=Fe)}$ [c]	0.00	0.30	0.61	0.34	0.65	0.00	0.03	0.04	0.24	0.65
μ_{O} [c]	-	-	-	-0.14	0.19	0.00	0.41	0.62	-0.01	0.08

[a] O=FeN$_4$. [b] O=FeN$_2$-trans. [c] O=FeN$_2$-cis.

Table S8 Magnetic moment of Fe and O in HO-FeN$_x$ and their intermediates in periodic models

Magnetic moment /μ_B	Bare active site		*OOH			*O		*OH		
	Doublet	Quartet	Singlet	Triplet	Quintet	Doublet	Quartet	Singlet	Triplet	Quintet
μ_{Fe} [a]	1.07	2.31	0.00	0.99	1.57	1.04	1.19	0.01	1.23	1.65
$\mu_{\mathrm{O\ (H\mathbf{O}\text{-}Fe)}}$ [a]	0.11	0.28	0.00	0.01	0.16	0.00	0.09	0.00	0.14	0.16
μ_{O} [a]	-	-	0.00	0.18	0.24	0.55	0.65	0.00	0.14	0.16
μ_{Fe} [b]	1.21	2.39	0.00	1.41	1.74	0.70	1.64	0.00	1.59	1.85
$\mu_{\mathrm{O\ (H\mathbf{O}\text{-}Fe)}}$ [b]	0.06	0.20	0.00	0.16	0.14	0.03	0.15	0.00	0.10	0.18
μ_{O} [b]	-	-	0.00	0.18	0.23	0.26	0.68	0.00	0.16	0.18
μ_{Fe} [c]	1.31	2.44	0.02	1.58	1.97	0.73	1.98	0.01	1.72	2.15
$\mu_{\mathrm{O\ (H\mathbf{O}\text{-}Fe)}}$ [c]	0.07	0.18	0.04	0.12	0.13	-0.01	0.08	0.15	0.13	0.16
μ_{O} [c]	-	-	-0.08	0.18	0.22	0.24	0.65	-0.13	0.13	0.16

[a] HO-FeN$_4$. [b] HO-FeN$_2$-trans. [c] HO-FeN$_2$-cis.

Table S9 Magnetic moment of Fe and O in FeN$_x$ and their intermediates in cluster models

Magnetic moment /μ_B	Bare active site			*OOH		*O			*OH	
	Singlet	Triplet	Quintet	Doublet	Quartet	Singlet	Triplet	Quintet	Doublet	Quartet
μ_{Fe} [a]	-0.04	1.85	1.99	0.88	2.11	-0.06	1.23	1.41	0.89	2.26
μ_{O} [a]	-	-	-	0.08	0.33	0.04	0.57	0.65	0.08	0.28
μ_{Fe} [b]	0.18	2.48	2.60	-0.07	1.58	0.00	0.68	1.77	0.34	1.65
μ_{O} [b]	-	-	-	0.03	0.08	0.00	0.27	0.50	0.00	0.11
μ_{Fe} [c]	0.09	2.48	2.65	1.51	1.75	0.00	0.75	1.98	1.73	1.80
μ_{O} [c]	-	-	-	0.10	0.07	0.00	0.35	0.52	0.13	0.11

[a] FeN$_4$. [b] FeN$_2$-trans. [c] FeN$_2$-cis.

Table S10 Magnetic moment of Fe and O in O=FeN$_x$ and their intermediates in cluster models

Magnetic moment /μ_B	Bare active site			*OOH		*O			*OH	
	Singlet	Triplet	Quintet	Doublet	Quartet	Singlet	Triplet	Quintet	Doublet	Quartet
μ_{Fe} [a]	-0.06	1.23	1.41	0.82	1.13	0.05	0.55	1.12	0.90	1.18
$\mu_{\mathrm{O\ (\mathbf{O}=Fe)}}$ [a]	0.04	0.57	0.65	0.59	0.64	-0.02	0.22	0.75	0.59	0.66
μ_{O} [a]	-	-	-	-0.03	0.14	0.00	0.19	0.75	0.04	0.06
μ_{Fe} [b]	0.00	0.68	1.77	0.58	0.70	0.00	1.00	0.73	0.67	0.71
$\mu_{\mathrm{O\ (\mathbf{O}=Fe)}}$ [b]	0.00	0.27	0.50	0.24	0.30	0.00	0.37	0.79	0.25	0.28
μ_{O} [b]	-	-	-	0.03	0.18	0.00	0.02	0.22	0.02	0.10
μ_{Fe} [c]	0.00	0.75	1.98	0.58	0.61	0.00	0.98	1.89	0.71	0.63
$\mu_{\mathrm{O\ (\mathbf{O}=Fe)}}$ [c]	0.00	0.35	0.52	0.28	0.48	0.00	0.42	0.55	0.31	0.40
μ_{O} [c]	-	-	-	-0.01	-0.08	0.00	0.01	0.09	-0.04	0.07

[a] O=FeN$_4$. [b] O=FeN$_2$-trans. [c] O=FeN$_2$-cis.

Table S11 Magnetic moment of Fe and O in HO-FeN$_x$ and their intermediates in cluster models

Magnetic moment /μ_B	Bare active site		*OOH			*O		*OH		
	Doublet	Quartet	Singlet	Triplet	Quintet	Doublet	Quartet	Singlet	Triplet	Quintet
μ_{Fe} [a]	0.89	2.26	0.00	1.13	1.63	0.90	1.19	0.00	1.32	1.82
$\mu_{\mathrm{O\ (H\mathbf{O}\text{-}Fe)}}$ [a]	0.08	0.28	0.00	0.10	0.16	0.04	0.06	0.00	0.13	0.15
μ_{O} [a]	-	-	0.00	0.18	0.28	0.59	0.66	0.00	0.13	0.15
μ_{Fe} [b]	0.34	1.65	0.00	1.37	1.44	0.67	0.71	-0.07	1.58	1.61
$\mu_{\mathrm{O\ (H\mathbf{O}\text{-}Fe)}}$ [b]	0.00	0.11	0.00	0.18	0.18	0.02	0.10	0.01	0.13	0.18
μ_{O} [b]	-	-	0.00	0.20	0.21	0.25	0.28	-0.08	0.16	0.15
μ_{Fe} [c]	1.73	1.80	0.00	1.55	1.67	0.71	0.63	-0.64	1.74	1.79
$\mu_{\mathrm{O\ (H\mathbf{O}\text{-}Fe)}}$ [c]	0.13	0.11	0.00	0.15	0.15	-0.04	0.07	-0.13	0.15	0.15
μ_{O} [c]	-	-	0.00	0.19	0.19	0.31	0.40	0.08	0.15	0.15

[a] HO-FeN$_4$. [b] HO-FeN$_2$-trans. [c] HO-FeN$_2$-cis.

Table S12 Bond distance of Fe-N, Fe-C and Fe-O of FeN$_x$ and their intermediates in both cluster and period models

Bond distance / Å	Bare active sites		*OOH		*O		*OH	
	Periodic	Cluster	Periodic	Cluster	Periodic	Cluster	Periodic	Cluster
d_{Fe-N} [a]	1.90	1.90	1.91	1.91	1.93	1.93	1.91	1.91
d_{Fe-O} [a]	-	-	1.78	1.78	1.65	1.65	1.82	1.82
$d_{Fe-N/C}$ [b]	1.91/1.90	1.93/1.91	1.97/1.93	1.96/1.91	1.99/1.94	1.98/1.92	1.97/1.94	1.95/1.90
d_{Fe-O} [b]	-	-	1.67	1.64	1.61	1.61	1.78	1.77
$d_{Fe-N/C}$ [c]	1.93/1.89	1.95/1.89	2.00/1.93	1.98/1.90	1.99/1.94	1.97/1.93	1.98/1.94	1.98/1.92
d_{Fe-O} [c]	-	-	1.79	1.80	1.60	1.61	1.77	1.80

[a] FeN$_4$. [b] FeN$_2$-trans. [c] FeN$_2$-cis.

Table S13 Bond distance of Fe-N, Fe-C and Fe-O of O=FeN$_x$ and their intermediates in both cluster and period models

Bond distance / Å	Bare active sites		*OOH		*O		*OH	
	Periodic	Cluster	Periodic	Cluster	Periodic	Cluster	Periodic	Cluster
d_{Fe-N} [a]	1.93	1.93	1.93	1.94	1.97	1.98	1.93	1.94
$d_{Fe=O}$ [a]	1.65	1.65	1.67	1.67	1.68	1.67	1.68	1.68
d_{Fe-O} [a]	-	-	1.96	1.93	1.68	1.67	1.92	1.92
$d_{Fe-N/C}$ [b]	1.99/1.94	1.98/1.92	1.97/1.93	1.96/1.94	1.90/2.20	1.87/2.23	1.96/1.93	1.97/1.94
$d_{Fe=O}$ [b]	1.61	1.61	1.63	1.61	1.64	1.63	1.62	1.62
d_{Fe-O} [b]	-	-	2.11	2.07	2.00	2.00	2.05	2.03
$d_{Fe-N/C}$ [c]	1.99/1.94	1.97/1.93	1.98/1.91	2.00/1.92	2.00/1.91	2.04/1.93	2.01/1.89	2.02/1.91
$d_{Fe=O}$ [c]	1.60	1.61	1.63	1.63	1.66	1.63	1.70	1.63
d_{Fe-O} [c]	-	-	1.95	1.93	1.66	1.94	1.94	1.90

[a] O=FeN$_4$. [b] O=FeN$_2$-trans. [c] HO-FeN$_2$-cis.

Table S14 Bond distance of Fe-N, Fe-C and Fe-O of HO-FeN$_x$ and their intermediates in both cluster and period models

Bond distance / Å	Bare active sites		*OOH		*O		*OH	
	Periodic	Cluster	Periodic	Cluster	Periodic	Cluster	Periodic	Cluster
$d_{\mathrm{Fe-N}}$ [a]	1.91	1.91	1.92	1.92	1.93	1.94	1.94	1.93
$d_{\mathrm{Fe-OH}}$ [a]	1.82	1.82	1.87	1.87	1.92	1.92	1.86	1.88
$d_{\mathrm{Fe-O}}$ [a]	-	-	1.83	1.86	1.68	1.68	1.86	1.88
$d_{\mathrm{Fe-N/C}}$ [b]	1.97/1.94	1.95/1.90	2.00/1.89	1.96/1.94	1.96/1.93	1.97/1.94	1.94/1.92	1.96/1.94
$d_{\mathrm{Fe-OH}}$ [b]	1.78	1.77	1.83	1.83	2.05	2.03	1.83	1.83
$d_{\mathrm{Fe-O}}$ [b]	-	-	1.88	1.87	1.62	1.62	1.89	1.88
$d_{\mathrm{Fe-N/C}}$ [c]	1.98/1.94	1.98/1.92	1.97/1.90	2.00/1.91	2.01/1.89	2.02/1.91	1.97/1.90	2.01/1.91
$d_{\mathrm{Fe-OH}}$ [c]	1.77	1.80	1.84	1.84	1.95	1.90	1.85	1.84
$d_{\mathrm{Fe-O}}$ [c]	-	-	1.87	1.87	1.70	1.63	1.85	1.84

[a] HO-FeN$_4$. [b] HO-FeN$_2$-trans. [c] HO-FeN$_2$-cis.

Table S15 The mean absolute error (MAE) and optimal overpotential obtained from scaling

	Models	Function (ΔU_1)	MAE	Optimal	
				Potential / V	η / V
PBE	Periodic	$\Delta U_1 = -1.01\Delta G_{*OH}+1.79$	0.048	0.89	0.34
	Cluster	$\Delta U_1 = -1.19\Delta G_{*OH}+2.00$	0.079	0.91	0.32
	Both	$\Delta U_1 = -1.06\Delta G_{*OH}+1.85$	0.077	0.90	0.33
PBE with Van der Waals interaction	Periodic	$\Delta U_1 = -1.01\Delta G_{*OH}+1.84$	0.047	0.92	0.31
	Cluster	$\Delta U_1 = -1.20\Delta G_{*OH}+2.03$	0.094	0.92	0.31
	Both	$\Delta U_1 = -1.06\Delta G_{*OH}+1.89$	0.088	0.92	0.31
PBE in implicit solvent	Periodic	$\Delta U_1 = -1.06\Delta G_{*OH}+1.87$	0.050	0.91	0.32
	Cluster	$\Delta U_1 = -1.33\Delta G_{*OH}+2.14$	0.112	0.92	0.31
	Both	$\Delta U_1 = -1.13\Delta G_{*OH}+1.95$	0.106	0.92	0.31
PBE with Van der Waals interaction in implicit solvent	Periodic	$\Delta U_1 = -1.06\Delta G_{*OH}+1.92$	0.063	0.93	0.30
	Cluster	$\Delta U_1 = -1.30\Delta G_{*OH}+2.11$	0.118	0.92	0.31
	Both	$\Delta U_1 = -1.13\Delta G_{*OH}+1.98$	0.104	0.93	0.30

References

1 J. K. Nørskov, J. Rossmeisl, A. Logadottir, L. Lindqvist, J. R. Kitchin, T. Bligaard and H. Jónsson, *J. Phys. Chem. B*, 2004, **108**, 17886-17892.

2 R. Christensen, H. A. Hansen, C. F. Dickens, J. K. Nørskov and T. Vegge, *J. Phys. Chem. C*, 2016, **120**, 24910-24916.